Plasma membrane translocation of REDD1 governed by GPCRs contributes to mTORC1 activation

Grégory Michel, Hans W D Matthes, Muriel Hachet-Haas, Keltouma El Baghdadi, Jan de Mey, Rainer Pepperkok, Jeremy C Simpson, Jean-Luc Galzi, Sandra Lecat

© 2014. Published by The Company of Biologists Ltd | Journal of Cell Science (2014) 127, 773–787 doi:10.1242/jcs.136432

RESEARCH ARTICLE

Plasma membrane translocation of REDD1 governed by GPCRs contributes to mTORC1 activation

Grégory Michel[1], Hans W. D. Matthes[1], Muriel Hachet-Haas[1], Keltouma El Baghdadi[1], Jan de Mey[2], Rainer Pepperkok[3], Jeremy C. Simpson[4], Jean-Luc Galzi[1] and Sandra Lecat[1,*]

ABSTRACT

The mTORC1 kinase promotes cell growth in response to growth factors by activation of receptor tyrosine kinase. It is regulated by the cellular energy level and the availability of nutrients. mTORC1 activity is also inhibited by cellular stresses through overexpression of REDD1 (regulated in development and DNA damage responses). We report the identification of REDD1 in a fluorescent live-imaging screen aimed at discovering new proteins implicated in G-protein-coupled receptor signaling, based on translocation criteria. Using a sensitive and quantitative plasma membrane localization assay based on bioluminescent resonance energy transfer, we further show that a panel of endogenously expressed GPCRs, through a Ca^{2+}/calmodulin pathway, triggers plasma membrane translocation of REDD1 but not of its homolog REDD2. REDD1 and REDD2 share a conserved mTORC1-inhibitory motif characterized at the functional and structural level and differ most in their N-termini. We show that the N-terminus of REDD1 and its mTORC1-inhibitory motif participate in the GPCR-evoked dynamic interaction of REDD1 with the plasma membrane. We further identify REDD1 as a novel effector in GPCR signaling. We show that fast activation of mTORC1 by GPCRs correlates with fast and maximal translocation of REDD1 to the plasma membrane. Overexpression of functional REDD1 leads to a reduction of mTORC1 activation by GPCRs. By contrast, depletion of endogenous REDD1 protein unleashes mTORC1 activity. Thus, translocation to the plasma membrane appears to be an inactivation mechanism of REDD1 by GPCRs, which probably act by sequestering its functional mTORC1-inhibitory motif that is necessary for plasma membrane targeting.

KEY WORDS: REDD1, mTOR, G-protein-coupled receptors, Bioluminescence resonance energy transfer, Ca^{2+}/calmodulin signaling pathway, Plasma membrane translocation

INTRODUCTION

One of the key mechanisms of signal transduction is a change in intracellular localization of signaling effectors. For example, the AKT/PKB kinase translocates from the cytoplasm to the plasma membrane upon activation of insulin receptor tyrosine kinase (Franke et al., 1997) and many transcription factors translocate from the cytoplasm to the nucleus upon receptor activation (Edwards, 1994). In recent years, the use of fluorescently conjugated signaling proteins has been instrumental in dissecting the spatio-temporal control of signaling pathways (Teruel and Meyer, 2000). Also, in pharmacology, they have been used to screen compound libraries for new drugs by high-content screening, for example in the G-protein-coupled receptor (GPCR) field, using plasma membrane translocation of the general effector β-arrestin2 as a read-out of GPCR activation (Hudson et al., 2006).

GPCRs form a structurally conserved family of plasma membrane receptors. They trigger intracellular signaling pathways by the activation of heterotrimeric G-proteins. Activated Gα and Gβ-γ complexes can transmit these signals to effectors, mainly enzymes or ion channels, leading to production of secondary messengers such as Ca^{2+} (for example through Gαq) or cAMP (Gαs-stimulatory and Gαi-inhibitory). A range of techniques, mostly focused on detecting interactions with GPCRs themselves, including proteomics and two-hybrid screening, have been used to identify the regulatory proteins within the diverse GPCR signaling pathways (Daulat et al., 2009).

We reasoned that screening a library of fluorescently modified proteins of unknown function for any changes in their intracellular localization upon GPCR activation might allow us to discover new protein components of the GPCR signaling pathways. Compared with interactome approaches, this alternative strategy permits us to directly address the question of spatial control of signaling in a dynamic manner.

We now present the successful identification of REDD1 during such a protein translocation screening procedure in living cells. REDD1, also known as RTP801/DDIT4/Dig2, is overexpressed under cellular stress (Ellisen, 2005). Genetic and biochemical studies have demonstrated that REDD1 functions in a tuberous sclerosis complex (TSC1/2)-dependent manner to negatively regulate the activity of mammalian target of rapamycin kinase mTORC1 governed by growth factors, leading to an arrest in protein synthesis and subsequent inhibition of cell growth (Ellisen et al., 2002; Brugarolas et al., 2004; Reiling and Hafen, 2004; Corradetti et al., 2005; DeYoung et al., 2008).

Although several GPCRs are implicated in the activation of mTORC1 (Musnier et al., 2010), no role for REDD1 in the GPCR signaling pathways has so far been described. Hence, we have characterized in a quantitative manner the kinetics of the translocation of REDD1 governed by GPCRs to determine to what extent REDD1 is a general effector of GPCR signaling and its possible functions in these pathways.

RESULTS

Screening for new modulators of GPCR signaling pathways

In order to identify new cytoplasmic proteins that can modulate GPCR signaling pathways, the Gq-coupled tachykinin NK2 receptor (NK2R) was chosen as a model. The screened library

[1]GPCRs, Pain and Inflammation Team, UMR7242, CNRS-University of Strasbourg, LabEx Medalis, 67412 Illkirch, France. [2]Cell Signaling Team, UMR 7213 CNRS-University of Strasbourg Faculty of Pharmacy, 67401 Illkirch, France. [3]European Molecular Biology Laboratory, Advanced Light Microscopy Facility, Meyerhofstrasse 1, 69117 Heidelberg, Germany. [4]School of Biology and Environmental Science & UCD Conway Institute, University College Dublin, Dublin 4, Ireland.

*Author for correspondence (sandra.lecat@unistra.fr)

Received 6 June 2013; Accepted 13 November 2013

Journal of Cell Science

Journal of Cell Science (2014) 127, 773–787 doi:10.1242/jcs.136432

was a fluorescent-tagged human full-length ORF plasmid collection from the GFP-cDNA localization project (Simpson et al., 2000). This plasmid collection is composed of ORFs of poorly characterized function that are fused in-frame with the cDNA encoding EYFP (enhanced yellow fluorescent protein).

In total, 183 fluorescent proteins from the library were selected for their intracellular cytoplasmic localization in resting cells and were screened. Each vector encoding one given fluorescent clone was transiently transfected for 24 hours in cells overexpressing NK2R. The live-cell screening procedure consisted for each individual clone of filming the activation process at different time-points. The criterion used to define a fluorescent protein as a positive clone was that, during the time-frame of 4 hours following activation of the NK2R with its agonist neurokinin A (NKA), the fluorescent protein was partly or entirely translocating from the cell cytoplasm to either the periphery of the plasma membrane, or into the nucleus, or towards intracellular membranes.

Fluorescently labeled β-arrestin2 (β-arr2–EYFP) and protein kinase C (PKC–EYFP) were used as positive controls during the screening procedure (Fig. 1A). β-arr2 is a cytoplasmic protein that translocates to the plasma membrane upon GPCR activation, interacts directly with many GPCRs including the NK2R, and serves primarily as an adaptor protein for clathrin (Hachet-Haas et al., 2006; Ouedraogo et al., 2008). Cytoplasmic PKC translocates to the plasma membrane following activation of Gq-coupled receptors and elevation of Ca^{2+} levels. At the plasma membrane, PKC is activated and phosphorylates the NK2R (Vollmer et al., 1999).

We observed that under basal conditions, transiently transfected β-arr2–EYFP or PKC–EYFP were visualized in the cytoplasm of cells, excluded from nuclei. Within seconds of addition of NKA, β-arr2–EYFP translocated to the plasma membrane, then after several minutes, appeared in vesicular structures that corresponded to early endosomes (Fig. 1A, Control 1 and supplementary material Movie 1) (Cézanne et al., 2004) whereas the PKC–EYFP fluorescent signal accumulated at the plasma membrane for less than 1 minute (Fig. 1A, Control 2 and supplementary material Movie 2).

REDD1 translocates to the plasma membrane upon activation of NK2R

The REDD1 protein was identified as a positive clone of the screen (Fig. 1A). Wild-type REDD1wt–mYFP was visualized in the cytoplasm and nucleus of cells before activation (Fig. 1A; supplementary material Movie 3). Several minutes after NKA addition, a proportion of REDD1wt–mYFP concentrated at the periphery of the cell, indicating translocation to the plasma membrane, and therefore identifying it as a potential modulator of NK2R signaling. First, we confirmed that the fusion of mYFP at the C-terminus of REDD1 preserves its function, by measuring the ability of C-terminally tagged REDD1 to inhibit mTORC1 signaling (supplementary material Fig. S1).

Following NK2R activation, the plasma membrane population of REDD1wt–mYFP was maintained over several minutes, but never appeared in vesicular structures (Fig. 1A and supplementary material Movie 3), suggesting that REDD1wt–mYFP does not follow the endocytosed NK2R, in contrast to β-arr2–EYFP.

To address a potential transient interaction between REDD1 and the NK2R before internalization of the receptor, as for PKC–EYFP, we made use of a bioluminescence resonance energy transfer (BRET1) assay in living cells (Fig. 1B). Because resonance energy transfer depends on the distance between the donor and the acceptor (which should range between 10 and 100 Å) and on their relative orientation, this technique detects interactions between proteins labeled with the Renilla luciferase (RLuc) as a donor of energy, and to the YFP as an acceptor of energy. Initially, the optimal conditions for detecting an agonist-promoted BRET signal were determined using the β-arr2–EYFP protein as a positive control. In particular, to avoid a non-specific BRET signal, minimal expression levels to detect a reproducible NKA-modulated BRET signal between the NK2R fused at its cytoplasmic tail to the RLuc protein (NK2R–RLuc), and β-arr2–EYFP, were determined. At 37°C, the BRET signal remained high for more than 1 hour, reflecting a stable interaction between β-arr2–EYFP and NK2R–RLuc in endosomes (Fig. 1B, left).

The same expression conditions for NK2R–RLuc were used to test both PKC–EYFP and REDD1wt–mYFP. For fluorescent protein expression analogous to β-arr2–EYFP, as detected by fluorescence measurement of the cells, a BRET signal between NK2R–RLuc could not be detected between PKC–EYFP or REDD1wt–mYFP when cells were incubated at 37°C. To detect a BRET1-interacting signal between PKC–EYFP and NK2R–RLuc, the reaction kinetic was slowed down by lowering the temperature of the assay to 28°C, then fast and transient NKA-induced BRET1 signals were recorded (Fig. 1B, middle). It was not possible to detect a NKA-induced BRET1 signal of interaction between REDD1wt-mYFP and the NK2R–RLuc at any temperature (Fig. 1B, right).

Hence, the timing and subcellular translocation of REDD1wt–mYFP suggest that REDD1 has a function in NK2R signaling although probably not by direct interaction with the receptors.

Measuring dynamic interactions of proteins with the plasma membrane in living cells using a quantitative and sensitive BRET assay

To test whether REDD1 translocated to the plasma membrane upon activation of other receptors, we set up a quantitative assay to measure plasma membrane localization in living cells (supplementary material Fig. S2). The assay consists of detecting proximity between a fluorescent plasma membrane marker (the myristoylated-palmitoylated-mYFP or Myr-Palm–mYFP) (Zacharias et al., 2002) and a protein that localizes at the plasma membrane expressed in fusion with RLuc by BRET. The overexpressed Myr-Palm–mYFP serves as a density-dependent BRET acceptor, with a BRET1 signal arising from the high effective concentration of Myr-Palm–mYFP confined to a two-dimensional plane, even in the absence of intermolecular affinity (BRET by collision) (Drake et al., 2008). With these lipid modifications, the Myr-Palm–mYFP was localized almost exclusively to the plasma membrane (supplementary material Fig. S2A).

As positive controls, high plasma membrane BRET signals were detected between the fluorescent plasma membrane marker Myr-Palm–mYFP and luminescently modified GPCRs, the tachykinin NK2R-RLuc, or the neuropeptide Y Y1 receptor (NPY1R-RLuc8), both known to reside at the plasma membrane and precise kinetics of internalization of activated receptors could be followed with this BRET assay (supplementary material Fig. S2B).

REDD1, but not its homolog REDD2, translocates to the plasma membrane upon activation of different endogenously expressed GPCRs

Having validated the plasma membrane localization BRET assay, the capacity of endogenously expressed receptors to modulate translocation of a luminescently modified REDD1, REDD1wt–RLuc8, was tested in

Journal of Cell Science (2014) 127, 773–787 doi:10.1242/jcs.136432

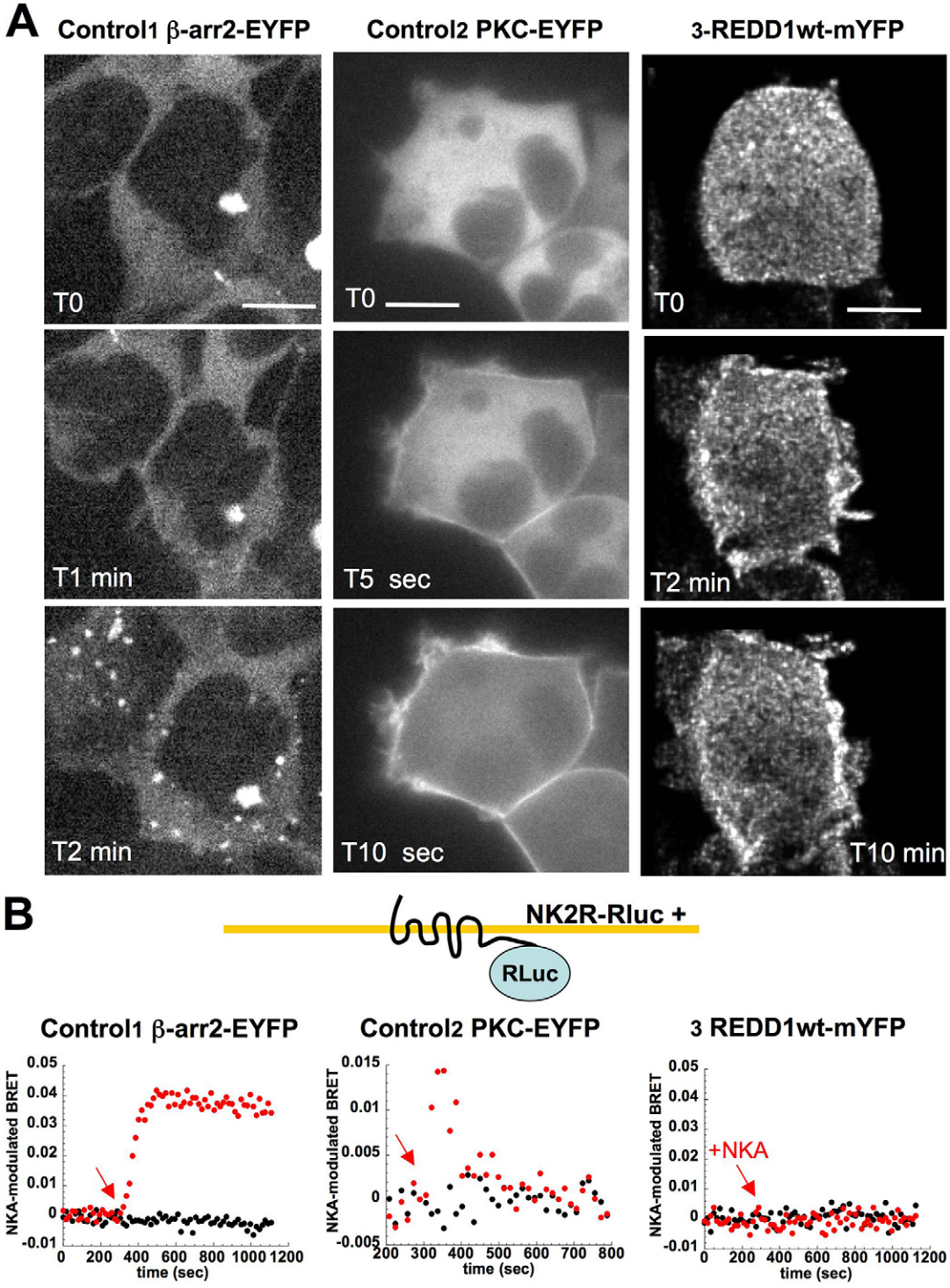

Fig. 1. REDD1 translocates to the plasma membrane upon NK2R activation, but does not interact directly with the receptor unlike β-arr2 or PKC. (A) Translocation to the plasma membrane of fluorescent proteins upon NK2R activation. Control1 β-arr2–EYFP, confocal images extracted from supplementary material Movie 1 with cells co-expressing NK2R and β-arr2–EYFP before (T0) or after activation with 100 nM neurokinin A agonist. Control2 PKC–EYFP, confocal images extracted from supplementary material Movie 2 presenting one *Z*-section of cells coexpressing NK2R and PKC–EYFP before (T0) or after activation. 3-REDD1wt-mYFP, 4D-fluorescent microscopy images extracted from supplementary material Movie 3 of one cell coexpressing NK2R and wild-type REDD1wt–mYFP before (T0) or after activation. Images are representative of three independent experiments. Scale bars: 5 μm. (B) BRET-interacting signal between β-arr2–EYFP or PKC–EYFP with NK2R–RLuc. Control1, kinetics of interaction between β-arr2–EYFP and NK2R–RLuc measured by BRET at 37°C. Control2, kinetics of interaction between PKC–EYFP and NK2R–RLuc measured by BRET at 28°C. 3-REDD1wt–mYFP, measurement of the BRET signal in cells overexpressing REDD1wt–mYFP together with NK2R–RLuc at 28°C as a function of time. Activation was performed with NKA (red dots) or vehicle (black dots) at 300 seconds. Representative data; $n=2$.

Journal of Cell Science (2014) 127, 773–787 doi:10.1242/jcs.136432

Myr-Palm–mYFP cells (Fig. 2) (Loening et al., 2006). HEK293 cells are particularly suitable for studying GPCR signaling because they endogenously express a significant diversity of GPCRs and their signaling partners (Shaw et al., 2002; Atwood et al., 2011) (supplementary material Table S1). We also confirmed that REDD1 is endogenously expressed in HEK293 cells (supplementary material Fig. S3A). For this study, we chose to analyze the effect of activating six endogenously expressed GPCRs: the Gq-coupled muscarinic M3 (M3R) and endothelin ET-B receptors (ETR), the Gs-coupled adenosine Ade2B (Ade2BR) and Beta-2adrenergic (Beta-2adrR) receptors, the Gi-coupled chemokine CXCR4 receptor and the G12-coupled Edg2 receptor (EdgR). We also tested two receptor tyrosine kinases (RTKs): the receptors for insulin growth factor (IGFR) and epidermal growth factor (EGFR).

Activation of the Gq-coupled M3R by acetylcholine (ACh, 10 μM) triggered a rapid agonist-induced BRET signal of REDD1wt–RLuc8 that reached a plateau value of ~0.02 at 400 seconds after activation (Fig. 2A, graph 1). Pre-incubation with the antagonist atropin (10 μM) for 30 minutes prevented M3R activation and translocation of REDD1 to the plasma membrane (Fig. 2A, graph 2). Similar kinetics of REDD1wt–RLuc8 agonist-induced BRET signal were observed when the Gq-coupled ETR was activated by endothelin (ET-1, 1 μM) (supplementary material Fig S2C, graphs 1,2). Activation of the Gs-coupled Ade2BR by NECA (1 μM) triggered a slow agonist-induced plasma membrane BRET signal of REDD1wt–RLuc8 that reached a plateau value of ~0.01 after 800 seconds (Fig. 2A, graph 3) and that was prevented by pre-incubation with specific antagonist (Fig. 2A, graph 4). Similar kinetics of increase in REDD1wt–RLuc8 plasma membrane BRET signal were observed when the Gs-coupled Beta-2adrR was activated by isoproterenol (Iso, 1 μM) (supplementary material Fig S2C, graphs 3,4). Activation of the Gi-coupled CXCR4 chemokine receptor by CXCL12 (100 nM) triggered a slow and modest agonist-induced BRET of REDD1wt–RLuc8 that reached a plateau value around 0.005 after 600 seconds (Fig. 2A, graph 5). The amplitude of the translocation was prevented by pre-incubation with CXCR4 antagonist AMD3100 (Fig. 2A, Graph 6). Of note, activation of the G12-coupled EdGR by lysophosphatidic acid (LPA, 1 μM) triggered no detectable translocation of REDD1 (supplementary material Fig S2C, graph 5).

Activation of RTKs – IGFR with insulin (10 μg/ml; Fig. 2B, graph 7) or EGFR with EGF (200 ng/ml) – did not promote translocation of REDD1wt–RLuc8 to the plasma membrane. As a control for the proper activation of IGFR, we confirmed translocation of AKT1–RLuc protein in the plasma membrane

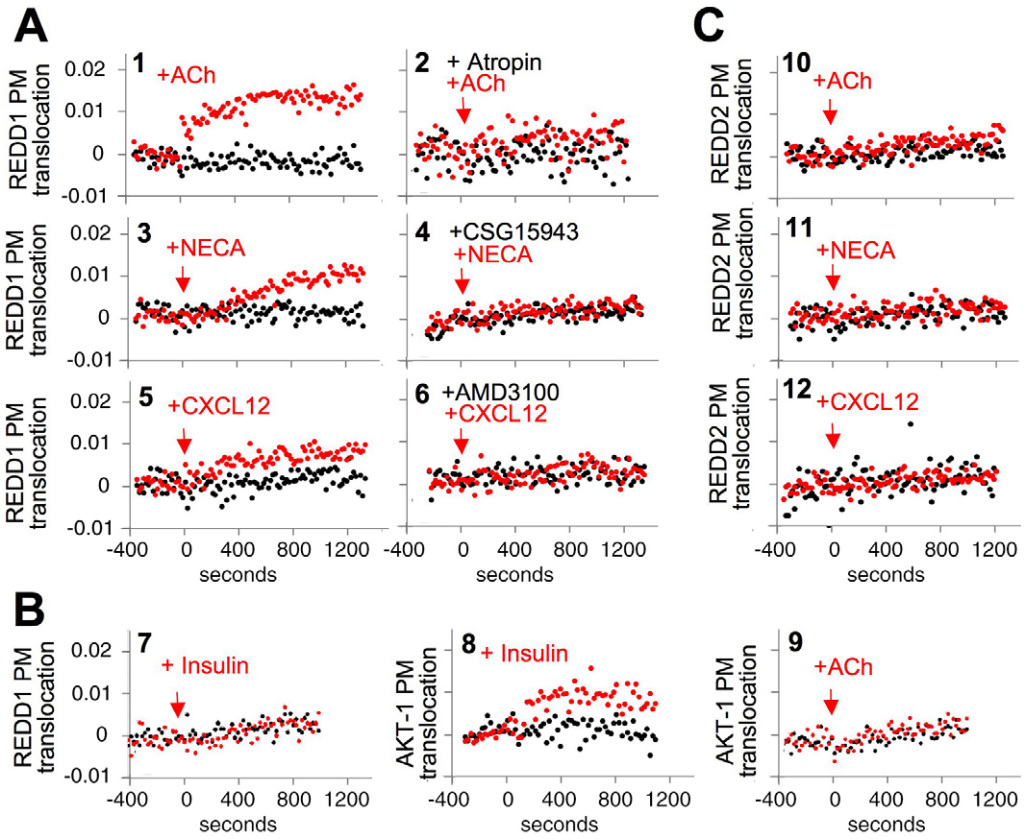

Fig. 2. REDD1 translocates to the plasma membrane upon activation of different endogenously expressed GPCRs but not upon IGFR activation. (A) GPCR activation triggers REDD1 translocation to the plasma membrane. Measurement of the agonist-induced plasma membrane BRET signal as a function of time in Myr-Palm–mYFP cells expressing REDD1wt–RLuc8. Activation of the Gq-coupled muscarinic M3 receptor with acetylcholine (ACh, red dots), Gs-coupled adenosine Ade2B receptor with NECA (red dots), and Gi-coupled chemokine CXCR4 receptor with CXCL12 (red dots), versus vehicle (black dots, control). Pre-treatment with antagonist was for 30 minutes (atropin or 10 μM CSG15943, 1 μM AMD3100). (B) AKT1, but not REDD1, translocates to the plasma membrane upon IGFR activation. Measurement of the insulin-induced plasma membrane BRET signal as a function of time in Myr-Palm–mYFP cells expressing REDD1wt–RLuc8 (graph 7) or AKT1-RLuc (graph 8). Graph 9, measurement of the ACh-induced plasma-membrane BRET signal as a function of time in Myr-Palm–mYFP cells expressing AKT1–RLuc. (C) REDD2 does not respond to GPCR activation. Measurement of the agonist-induced plasma membrane BRET signal as a function of time in Myr-Palm–mYFP cells expressing REDD2–RLuc8. Kinetics recorded at 37°C. Activation was performed at time 0. Representative data, $n=3$.

Journal of Cell Science (2014) 127, 773–787 doi:10.1242/jcs.136432

BRET assay. IGFR activation with insulin triggered a significant agonist-induced BRET of AKT1–RLuc that reached a plateau value of ~0.01 after 400 seconds (Fig. 2B, graph 8). Of note, AKT1–RLuc did not respond to any GPCR activation in this assay (for example, ACh activation in Fig. 2B, graph 9). Like REDD1, its homolog REDD2 (57% sequence identity), has been found to inhibit mTORC1 activity (Corradetti et al., 2005; Miyazaki and Esser, 2009). However, in the plasma membrane BRET assay, REDD2 fused to RLuc8 (REDD2–RLuc8), did not respond to any GPCR activation (Fig. 2C), suggesting that there is an as yet unidentified functional difference between the two proteins. In conclusion, these data clearly establish that REDD1 is a common component of GPCR signaling because its translocation to the plasma membrane is regulated by several different GPCRs, but not by RTKs.

Translocation of REDD1 to the plasma membrane is triggered by a GPCR–Ca^{2+}/calmodulin pathway

Next, we investigated the common signaling event responsible for plasma membrane translocation of REDD1 (Fig. 3). The intracellularly active Ca^{2+} chelator, BAPTA-AM (20 µM, 2 hours), completely blocked agonist-induced plasma membrane translocation of REDD1wt–RLuc8 (Fig. 3A). This led us to analyse Ca^{2+} responses to the different agonists (supplementary

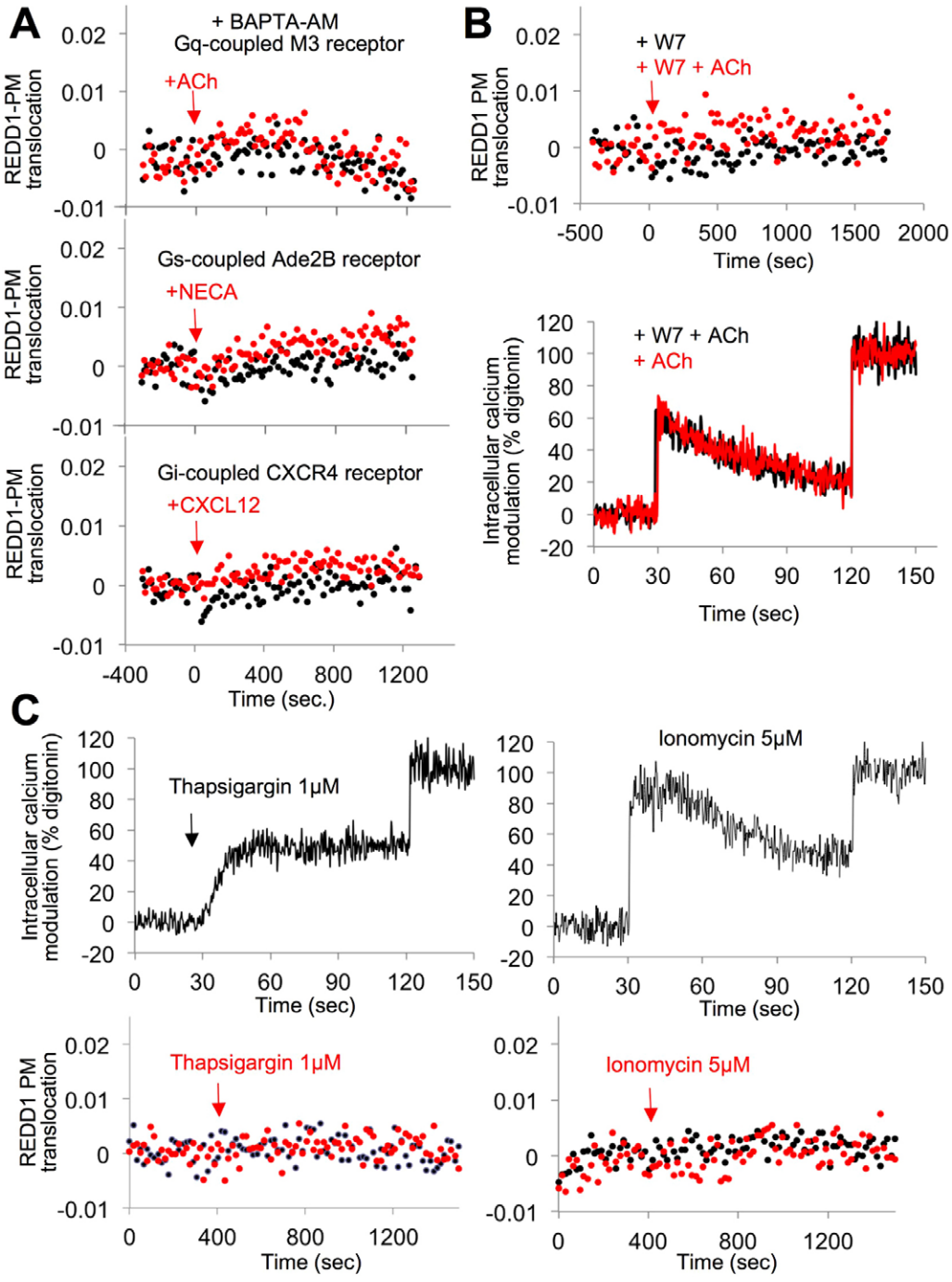

Fig. 3. A GPCR-mediated Ca^{2+}/calmodulin signaling pathway to translocate REDD1 to the plasma membrane. (A) REDD1wt–RLuc8 translocation is inhibited by intracellular Ca^{2+} chelation. Measurements of the agonist-induced plasma membrane BRET signal as a function of time in Myr-Palm–mYFP cells expressing REDD1wt–RLuc8. Cells were pre-treated for 2 hours with BAPTA-AM (red dots, BAPTA-AM then agonist at time 0; black dots, BAPTA-AM, then vehicle). (B) Calmodulin inhibition blocks REDD1 translocation. Top, measurement of the ACh-induced plasma membrane BRET signal as a function of time in Myr-Palm–mYFP cells expressing REDD1wt–RLuc8. Cells were pre-treated with W7 and activated (red) or not (vehicle, black). Bottom, intracellular Ca^{2+} peak induced at 30 seconds by ACh (red) or in cells pre-treated with W7 for 20 minutes before ACh activation (black) as a function of time. (C) An intracellular increase in Ca^{2+} concentration is not sufficient to translocate REDD1. Top, Ca^{2+} responses generated at 30 seconds with thapsigargin or ionomycin. Bottom, measurement of the ionophore-induced plasma membrane BRET signal as a function of time in Myr-Palm–mYFP cells expressing REDD1wt–RLuc8. Representative data, $n=3$.

Journal of Cell Science (2014) 127, 773–787 doi:10.1242/jcs.136432

material Fig. S3C). We observed that, not only did Gq-coupled receptors induce an elevation of intracellular Ca^{2+} concentration when stimulated at 37℃, but that detectable Ca^{2+} responses were also generated by Gs-coupled Ade2BR and Beta-2adrR and the Gi-coupled CXCR4 (supplementary material Fig. S3C). Furthermore, for each agonist, the amplitude of the maximal Ca^{2+} response was correlated with the maximal agonist-induced plasma membrane BRET signal of REDD1wt–RLuc8 (supplementary material Fig. S3D).

Pre-treatment of cells for 20 minutes with the calmodulin inhibitor W7 (25 µM), completely abolished ACh-induced plasma membrane BRET translocation of REDD1wt–RLuc8 (Fig. 3B, top panel) without altering the ACh-induced Ca^{2+} response (Fig. 3B, bottom panel). Importantly, Ca^{2+} alone was not sufficient for translocation of REDD1wt–RLuc8, because an increase of intracellular Ca^{2+} concentration generated by thapsigargin (1 µM), or by ionomycin (5 µM), had no effect on localization of REDD1wt–RLuc8 (Fig. 3C). Taken together, these results strongly suggest that REDD1 translocation is specifically mediated by GPCRs through Ca^{2+}/calmodulin signaling.

REDD1 but not REDD2 is associated with the plasma membrane under basal conditions

We observed a clear difference in the GPCR-regulated intracellular localization of REDD1 compared with REDD2 (Fig. 4). Under basal conditions, the BRET ratio between the plasma membrane marker, Myr-Palm–mYFP, and REDD1wt–RLuc was very high (Fig. 4A). This BRET ratio was specific, because it was not observed between the REDD1wt–RLuc and the fluorescent negative control proteins YFP–actin or Gbeta–YFP (Ouedraogo et al., 2008) when they were expressed at a similar level as Myr-Palm–mYFP. REDD1 is reported to be mainly localized in the cytoplasm and the nucleus (Simpson et al., 2000, Lin et al., 2005) but it has also been observed in a membrane fraction (DeYoung et al., 2008). The BRET results suggest that, in resting cells, a non-negligible fraction of REDD1 is associated with the plasma membrane. In Fig. 4B, the specific

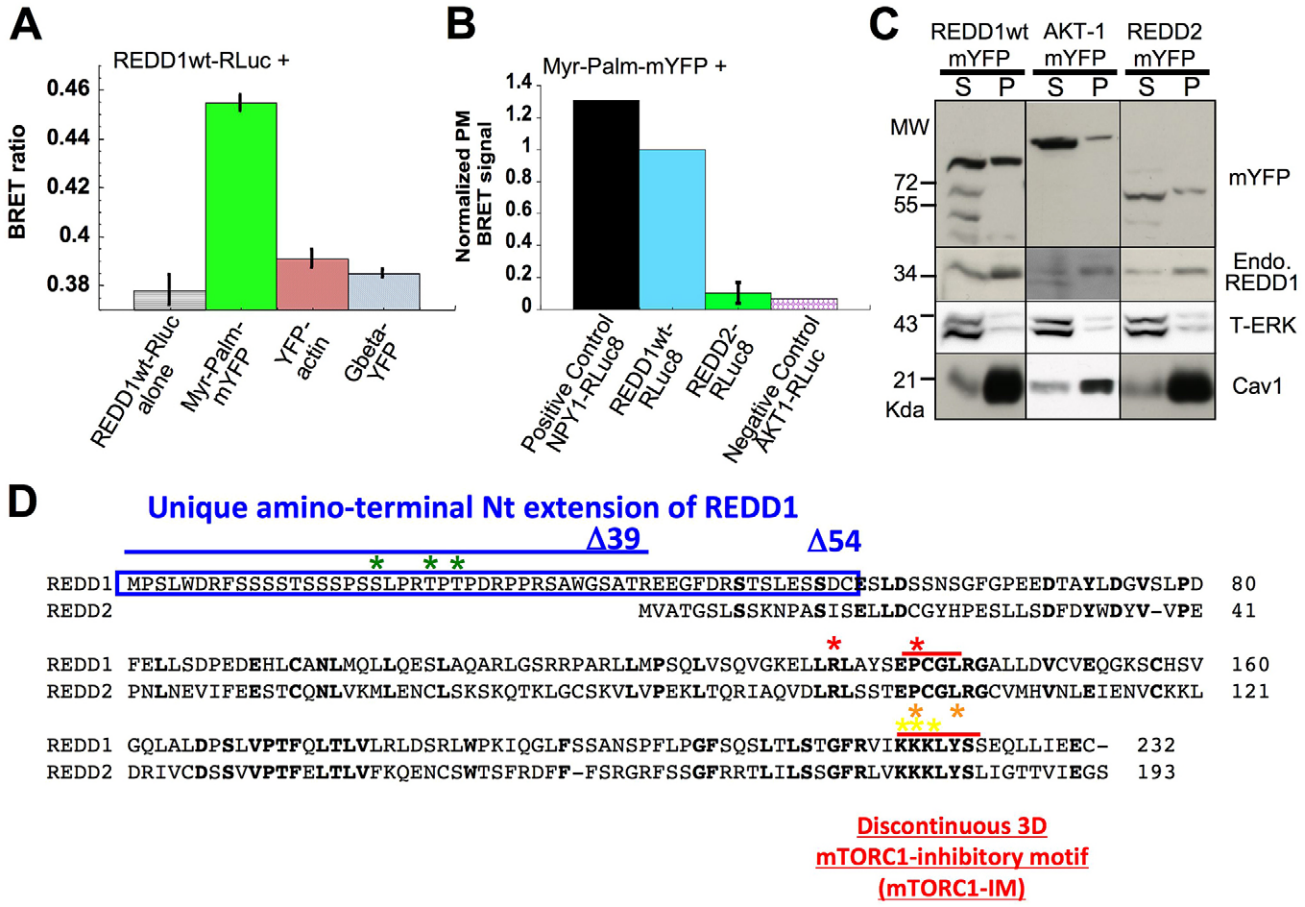

Fig. 4. REDD1, but not its homolog REDD2, is associated with the plasma membrane in resting cells. (A) A large and specific BRET signal indicating proximity between REDD1wt–RLuc and the plasma membrane Myr-Palm-mYFP. BRET ratio measured in cells coexpressing REDD1wt-RLuc with Myr-Palm-mYFP, negative controls YFP–actin or Gbeta-YFP compared with REDD1wt–RLuc-alone (no YFP BRET acceptor). $n=2$ in duplicate ± s.d. (B) Plasma membrane net BRET signal for REDD1 compared with positive and negative controls, plasma membrane NPY1R and cytoplasmic AKT1, respectively. Plasma membrane net BRET is normalized to 1 for Myr-Palm–mYFP cells expressing REDD1wt–RLuc8. $n=2$ in duplicate ± s.d. (C) REDD1 associates with the membrane pellet fractions. Supernatant (S) and pellet (P) ultracentrifugation fractions of post-nuclear supernatants were processed for western blot analysis. Western blots were probed with anti-GFP antibodies to detect REDD1–mYFP or the negative controls AKT1–mYFP or REDD2–mYFP. The same fractions were probed with anti-REDD1 antibodies to detect endogenous REDD1, with total-ERK antibodies to detect the cytosolic fraction and with antibodies against caveolin 1 to detect the membrane fraction (Cav1). Representative data, $n=2$. (D) Amino acid sequence alignment between human REDD1 and REDD2 including the mutated residues.

net BRET signal between REDD1wt–RLuc8 and Myr-Palm–mYFP was normalized to 1 for comparative purposes. The level of net BRET signal of the plasma membrane positive control NPY1R–RLuc8 receptor with Myr-Palm–mYFP was similar (Fig. 4B). In resting cells, AKT1–RLuc gave a plasma membrane net BRET signal only marginally above background, as expected for a cytoplasmic protein (Fig. 4B). Furthermore, for similar levels of expression, REDD2–RLuc8 did not show a plasma membrane net BRET signal (Fig. 4B).

A membrane fractionation assay was used to further support the finding that REDD1 associates with membranes (Fig. 4C). When analyzed by western blotting, overexpressed REDD1wt–mYFP could be detected both in the cytosolic supernatant and in the 100,000 ***g*** membrane pellet of post-nuclear supernatant extracts, with ERK and caveolin 1 used as endogenous cytosolic and membrane markers, respectively (Fig. 4C). Overexpressed AKT1–mYFP and REDD2–mYFP were predominantly found in the cytosolic fraction. In the same fractionation assay, endogenous REDD1 was enriched in the membrane pellet (Fig. 4C and supplementary material Fig. S3B). Taken together with the plasma membrane BRET assay, the data indicate that under basal conditions, a proportion of REDD1 associates with the plasma membrane, whereas its homolog REDD2 does not.

The unique N-terminal domain of REDD1 contributes to dynamic interaction of REDD1 with the plasma membrane

To identify the residues of REDD1 responsible for plasma membrane association and regulation by GPCRs, we generated several mutants (Fig. 4D and supplementary material Table S2). At the primary sequence level, REDD2 mostly differs from REDD1 in the N-terminus (Nt) up to residue 54 of REDD1. In particular, REDD1 possesses a 39 amino acid extension. To address the role of this Nt domain, two deletion mutants Δ39 and Δ54 were generated. These Nt-mutants were then fused, either to mYFP and then expressed in stable clonal cell lines for subcellular localization (Fig. 5A) and biochemical membrane fractionation (Fig. 5B), or to RLuc8 and transiently transfected for the plasma membrane BRET assay (Fig. 5C and Fig. 6A).

Under basal conditions, confocal image analysis detected these fluorescent Nt-mutants in the cytoplasm and the nucleus (Fig. 5A). By membrane fractionation, both Δ39-REDD1–mYFP and Δ54-REDD1–mYFP partitioned equally in the supernatant and membrane pellet (Fig. 5B). Under basal conditions, in the plasma membrane BRET assay (Fig. 5C), the two deletions yielded different phenotypes. For similar levels of expression, Δ39-REDD1–RLuc8 gave 60% of the signal of

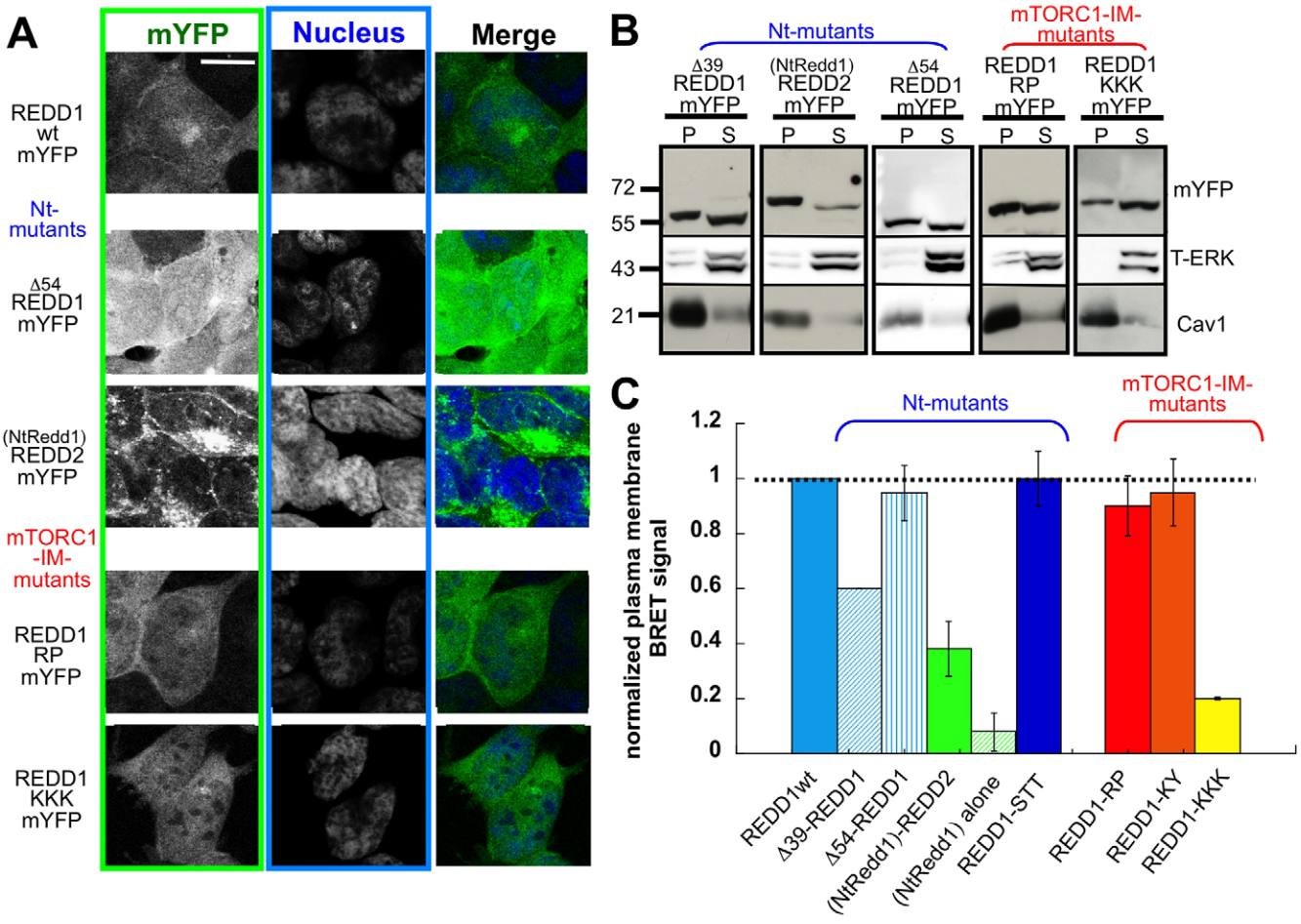

Fig. 5. The unique Nt of REDD1 and its mTORC1-inhibitory motif both contribute to plasma membrane association in resting cells. (A) Intracellular localization of fluorescent Nt- or mTORC1-IM-mutants of REDD proteins. Confocal images taken in the middle of the *Z*-axis of cells are presented. mYFP fluorescence (left). Nuclei are stained with Hoechst (middle). Merge of the two images (right). (B) Membrane localization of fluorescent Nt- or mTORC1-IM-mutants of REDD proteins as measured by ultracentrifugation (as in Fig. 4C). Representative data, $n=3$. (C) Plasma membrane localization measured by BRET of luminescent Nt- or mTORC1-IM-mutants of REDD proteins (as in Fig. 4B). Experimental results are presented with s.d. and were performed in duplicate, $n=3$.

Journal of Cell Science (2014) 127, 773–787 doi:10.1242/jcs.136432

REDD1wt–RLuc8, but the truncation of 15 additional residues restored the plasma membrane BRET signal (Fig. 5C). In the REDD1 sequence, the 15 residues after this Nt domain might carry a membrane association inhibitory motif that is masked by the 39 first residues.

In their response to GPCRs in the plasma membrane BRET assay (Fig. 6A), the two deletion mutants behaved identically: the amplitude of the REDD1 translocation governed by M3R was reduced by half (Fig. 6A, graph 1 for Δ39-REDD1–RLuc8) and no translocation was detected for Gs- or Gi-coupled receptor activation. We also generated a mutant in the Nt of REDD1, by replacing the three major phosphorylated residues described previously, i.e. Ser19, Thr23 and Thr 25, with alanine (Fig. 4D and supplementary material Table S2) (Katiyar et al., 2009). In resting cells, for similar levels of expression, the mutant REDD1-STT–RLuc8 yielded a plasma membrane BRET signal identical to REDD1wt (Fig. 5C). This also translocated with the same kinetics and amplitudes as REDD1wt upon activation of the cells with ACh (Fig. 6A, graph 2). Thus, these Nt residues were not necessary for membrane localization of REDD1.

To further explore the role of the Nt of REDD1 in plasma membrane targeting, we fused the first 39 residues of REDD1 onto REDD2 (supplementary material Table S2). Under basal conditions, (NtRedd1)-REDD2–mYFP was detected at the periphery of the cell and in numerous intracellular vesicular structures (Fig. 5A). In agreement, the (NtRedd1)-REDD2–mYFP protein also became predominant in the 100,000 ***g*** pellet (Fig. 5B). In addition, (NtRedd1)-REDD2–RLuc8 gave a significant plasma membrane BRET signal (Fig. 5C) compared with less than 10% for REDD2 (Fig. 4B). The plasma membrane BRET signal was 30% of REDD1wt, probably because the chimeric protein localized to other membrane compartments in addition to the plasma membrane. The Nt of REDD1 could also trigger plasma membrane translocation of (NtRedd1)-REDD2–RLuc8 upon M3R activation although to a lesser extent than REDD1wt–RLuc8 (Fig. 6A, graph 3), which is probably why no translocation was detected for Gs- or Gi-coupled receptor activation. Importantly, the Nt of REDD1 alone fused to RLuc8 [(Nt-Redd1)–RLuc8] did not trigger RLuc8 association with the plasma membrane (Fig. 5C) nor its response to GPCR activation (Fig. 6A, graph 4 illustrated for ACh). Thus, the unique Nt domain of REDD1 confers plasma membrane association to REDD2 and sensitizes it to GPCR activation, but is not sufficient for membrane targeting and translocation of REDD1 evoked by GPCRs, suggesting that other domains of REDD1 contribute as well.

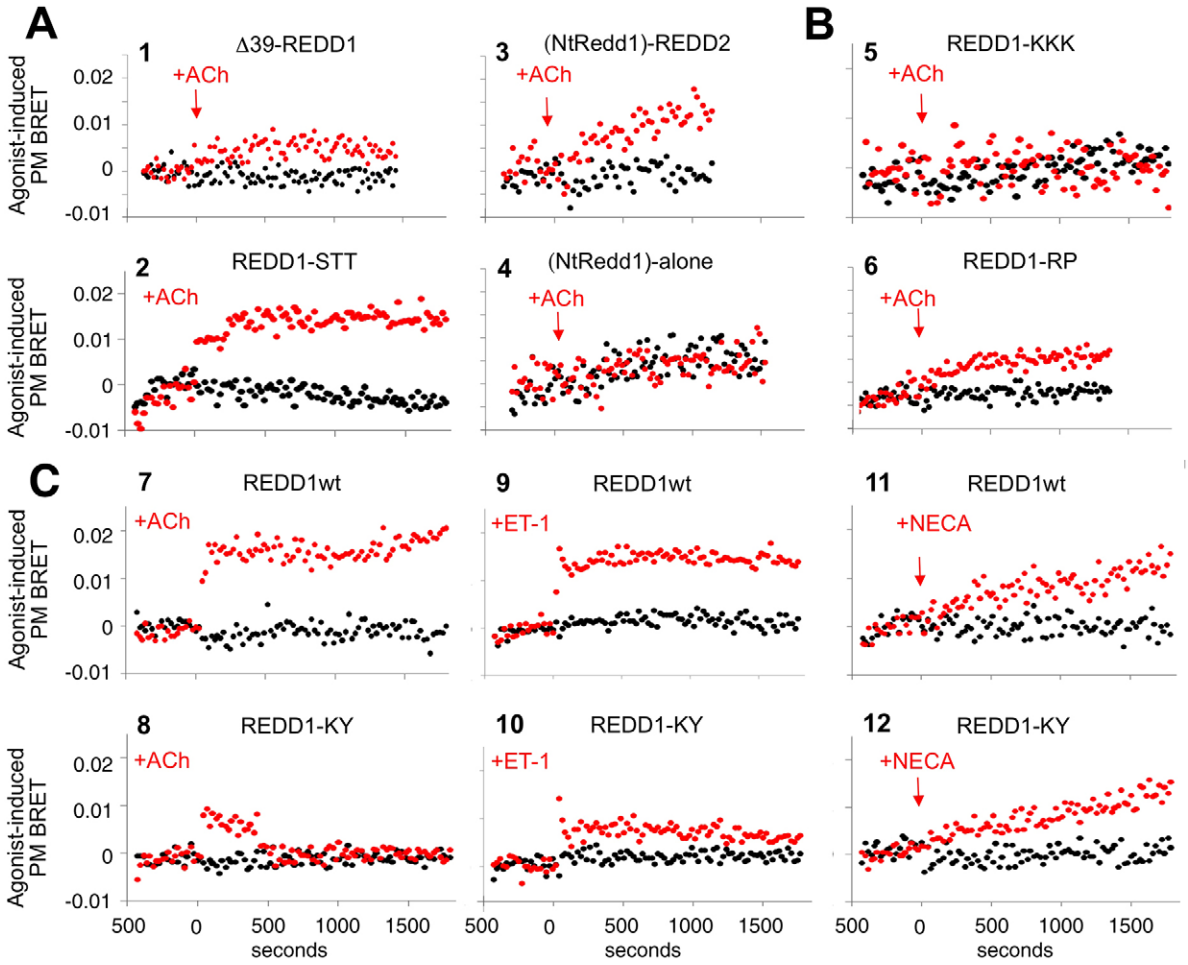

Fig. 6. The unique Nt of REDD1 and its mTORC1-inhibitory motif both participate in REDD1 translocation upon GPCR activation. Measurements of the ACh-induced plasma membrane BRET signal as a function of time in Myr-Palm–mYFP cells expressing Nt-mutants (A) or mTORC1-IM-mutants (B) of REDD proteins. (C) Comparison of the kinetics of plasma membrane BRET translocation of REDD1wt and REDD1-KY upon activation of cells with acetylcholine, endothelin or NECA (as in Fig. 2).

Journal of Cell Science (2014) 127, 773–787 doi:10.1242/jcs.136432

The mTORC1-inhibitory motif of REDD1 is necessary for plasma membrane association and contributes to REDD1 translocation upon GPCR activation

The structure of the most conserved domain found in REDD1 and REDD2 extends from amino acids 88 to 228 in REDD1, and is unique among the known three-dimensional structures listed in the Protein Data Bank database (Vega-Rubin de Celis et al., 2010). Within the REDD1 fold, a conserved non-linear functional 'hot spot', including residues 138–141 and 218–223 of REDD1 has been structurally delineated as a motif necessary for mTORC1 inhibition; we refer to this as the 'mTORC1-inhibitory motif' in the following text (mTORC1-IM, Fig. 4D). We generated three mutants in this motif by alanine replacement (supplementary material Table S2): REDD1-RP and REDD1-KY are known loss-of-function mutants for mTORC1 regulation (Vega-Rubin de Celis et al., 2010). REDD1-KKK was another mutant of the mTORC1-IM used in this study.

In resting cells, confocal image analysis of stable cell lines expressing these fluorescent mTORC1-IM mutants revealed a diffuse fluorescence in the nucleus and the cytoplasm, as seen for REDD1wt–EYFP (Fig. 5A, mTORC1-IM mutants). Western blot analysis of cell lysate subfractions (Fig. 5B, mTORC1-IM mutants) showed that the REDD1-RP–mYFP proteins segregated equally between cytosolic and membrane fractions, similar to REDD1wt–mYFP, but that the REDD1-KKK–mYFP proteins were predominant in the cytosolic fraction (70±10% cytosolic versus 45±5% for the wt). Accordingly, the REDD1-RP–RLuc8 and the REDD1-KY–RLuc8 mutants were not altered in their plasma membrane BRET signal (Fig. 5C, mTORC1-IM mutants), in contrast to the REDD1-KKK–RLuc8, which gave a plasma membrane BRET signal of only 20% of the REDD1wt–RLuc8 in resting cells.

In addition, all the mTORC1-IM mutants of REDD1 had defects in their translocation governed by GPCRs, but to different extents (Fig. 6B): the cytosolic REDD1-KKK–RLuc8 did not respond to any GPCR (Fig. 6B, graph 5 for ACh activation), REDD1-RP–RLuc8 responded to GPCRs, but the kinetics of translocation was slower and the amplitude of the plasma membrane-induced BRET was smaller for ACh activation (Fig. 6B, graph 6) and almost undetectable with other agonists (supplementary material Fig. S4A).

Interestingly, REDD1-KY–RLuc8 had rapid, but transient kinetics of translocation upon Gq-coupled M3R activation, never reaching the plateau (compare Fig. 6C, graph 8 with the wt signal recorded concomitantly in graph 7). This transient translocation of REDD1-KY–RLuc8 was also observed by stimulating cells with Gq-coupled ETR (compare Fig. 6C, graph 10 with the wt signal graph 9). Surprisingly, when cells were activated with Gs-coupled Ade2BR, the REDD1-KY–RLuc8 mutant presented the same kinetics of plasma membrane translocation as REDD1wt–RLuc8 (compare Fig. 6C, graphs 12 and 11, respectively).

In conclusion, the results clearly indicate that a triple lysine stretch from the mTORC1-inhibitory motif of REDD1 is necessary for plasma membrane association and that other residues of the mTORC1-IM participate in the GPCR-evoked translocation of REDD1 to the plasma membrane. If the mTORC1-IM of REDD1 is engaged in plasma membrane targeting, it might not be available for inhibition of the mTORC1 complex.

Fast mTORC1 activation by GPCRs correlates with rapid and robust translocation of REDD1 to the plasma membrane

Several reports mention a role for GPCRs in activating mTORC1. Growth factors stimulate mTORC1 signaling through RTKs that activate the PI3K/AKT signaling pathway. AKT phosphorylates TSC2 at multiple sites, releasing the inhibitory effect of the TSC1/2 complex, and resulting in the activation of mTORC1 signaling (Inoki et al., 2002) (Fig. 7A). REDD proteins activate the TSC1/2 complex to subsequently inhibit mTORC1. To elucidate the functional link between GPCR-induced REDD1 translocation to the plasma membrane and GPCR signaling, we tested which endogenously expressed GPCRs were triggering mTORC1 activation. To monitor mTORC1 kinase activation, we analyzed the activity of a direct and specific substrate of mTORC1, the p70-S6K kinase, through its phosphorylation of the ribosomal subunit S6 (S6R). To do this, we used two specific monoclonal antibodies that recognise two phosphorylated pairs of serines on S6R, residues Ser235/6 and residues Ser240/4, respectively (Fig. 7A).

We found that only the Gq-coupled M3R and ETR induced a significant phosphorylation on both serine pairs of S6R indicating mTORC1 activation, as early as 5 minutes after activation (Fig. 7B,C). These kinetics of mTORC1 activation correlate with the kinetics of translocation of REDD1 governed by these receptors. Although Gs-coupled Ade2BR and Beta-2adrR both induced a significant phosphorylation within 5 minutes of activation on Ser235/6, phosphorylation on Ser240/4 was not increased (Fig. 7B,C) as for activated Gi-coupled CXCR4. This suggests no detectable activation of mTORC1 in the first 30 minutes post-activation of Gs- and Gi-coupled receptors. Because all the agonists tested led to early phosphorylation of extracellular signal-regulated kinase 1/2 (ERK1/2), phosphorylation of S6R235/6 could result from activation of ribosomal S6K kinase (p90-RSK) through ERK rather than p70-S6K through mTORC1 (Fig. 7A) (Roux et al., 2007).

In agreement with the absence of AKT1–RLuc translocation (Fig. 2B, graph 9), mTORC1 activation by Gq-coupled receptors did not seem to occur by the classical PI3K/AKT phosphorylation pathway, because AKT did not become phosphorylated upon activation of the cells with ACh or ET-1 (Fig. 7B). Conversely, the positive control, insulin, triggered detectable levels of phosphorylation of AKT. In addition, the kinetics of mTORC1 activation by insulin was slower than by Gq-coupled receptors, appearing only after 15 minutes of activation (Fig. 7B). In conclusion, fast mTORC1 activation occurs for those GPCRs that induce fast and large translocation of REDD1 to the plasma membrane.

A basal level of REDD1 inhibits mTORC1 in HEK293 cells

Several reports show that depletion of REDD1 *in vitro* or *in vivo* causes an increase in basal mTORC1 activity (Sofer et al., 2005; Corradetti et al., 2005; Noseda et al., 2013), suggesting that basal expression of REDD1 already has an inhibitory effect on mTORC1. In particular the strong activation of mTORC1 governed by the mRNA translation inhibitor cycloheximide has been directly linked to the loss of REDD1 protein owing to its rapid degradation, because the cycloheximide-induced increase in mTORC1 signaling was significantly attenuated in REDD1$^{-/-}$ MEF cells (Kimball et al., 2008).

In order to test whether the level of endogenous expression of REDD1 in HEK293 cells was also sufficient to inhibit mTORC1 activity, we thus made use of the short half-life of REDD1: serum-starved cells were treated with a 12-minute pulse of cycloheximide (CHX, 50 μM), which caused the disappearance of endogenous REDD1 (Fig. 8A). This fast loss of REDD1, without any activation of GPCRs, correlated with a rapid and

Journal of Cell Science (2014) 127, 773–787 doi:10.1242/jcs.136432

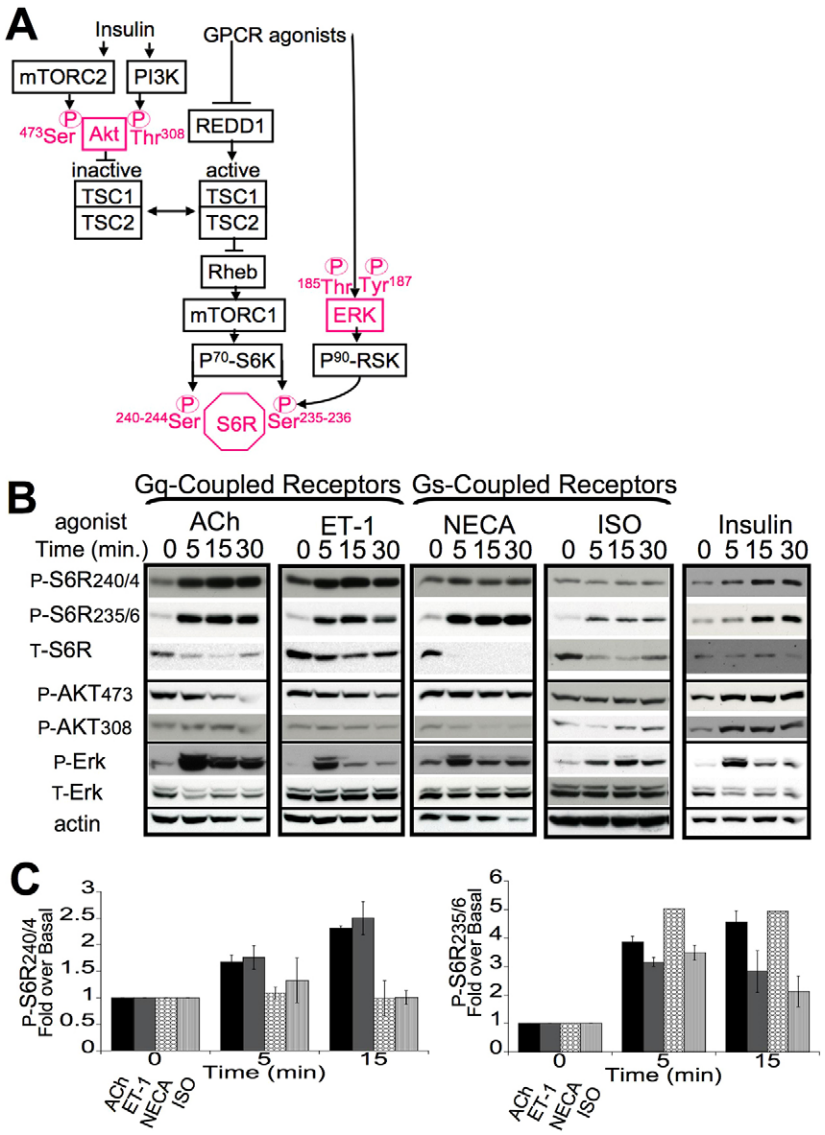

Fig. 7. Gq-coupled receptors activate mTORC1. (A) Schematic representation of the signaling pathways linking inhibition of REDD1 by GPCRs to mTORC1 activation. Proteins analyzed for phosphorylation are in pink. (B) Western blots of cell extracts after overnight serum starvation and agonists activation up to 30 minutes. Representative data, $n=3$. (C) Quantification of P-S6R over basal, $n=2$; results are means ± s.d.

strong phosphorylation of S6R, reflecting mTORC1 activation (Fig. 8A, Time 0). CHX treatment had no effect on basal levels of P-AKT or P-ERK.

Activation of cells with ACh after CHX treatment drastically increased mTORC1 activity. Of note, mTORC1 was the only tested signaling pathway activated by M3R that was affected by CHX; the increase in ERK phosphorylation was unaltered (Fig. 8A), as were the kinetics and amplitude of Ca^{2+} responses triggered by this Gq-coupled receptor (supplementary material Fig. S4B). In the absence of REDD1 as a result of CHX treatment, activation of Gq-coupled receptors M3R and ETR still triggered an increased phosphorylation on Ser240/4 of S6R compared with CHX treatment alone (Fig. 8B). Interestingly, in the absence of REDD1, activation of Gs-coupled Ade2BR and Beta-2adrR triggered a detectable increase in phosphorylation on Ser240/4 of S6R compared with CHX treatment alone. Thus, endogenous levels of REDD1 in HEK293 cells could be sufficient to exert an inhibitory effect on mTORC1 activity. Therefore a mechanism that contributes to the inhibition of REDD1 might be necessary for GPCRs to significantly activate mTORC1.

Overexpression of functional REDD1–mYFP reduces mTORC1 activity regulated by GPCRs

Inversely, although Ca^{2+} responses to ACh were unaltered in cells stably overexpressing REDD1wt–mYFP (supplementary material Fig. S4B), phosphorylations of S6R were reduced upon activation of Gq-coupled M3R (Fig. 8C) or ETR. Cells overexpressing Δ54-REDD1–mYFP also presented a reduction of agonist-induced mTORC1 function. Cells expressing REDD1-KKK–mYFP activated mTORC1 to the same extent as untransfected cells, illustrating that mutation of these three lysines generate another loss-of-function mutant towards mTORC1 modulation. Cells overexpressing functional REDD1 also presented a reduced phosphorylation of S6R235/6 induced by Gs-coupled Ade2BR (Fig. 8D) and Beta-2adrR. This phenotype could be attributed to a reduction in the basal mTORC1 activity owing to overexpressed REDD1.

Journal of Cell Science (2014) 127, 773–787 doi:10.1242/jcs.136432

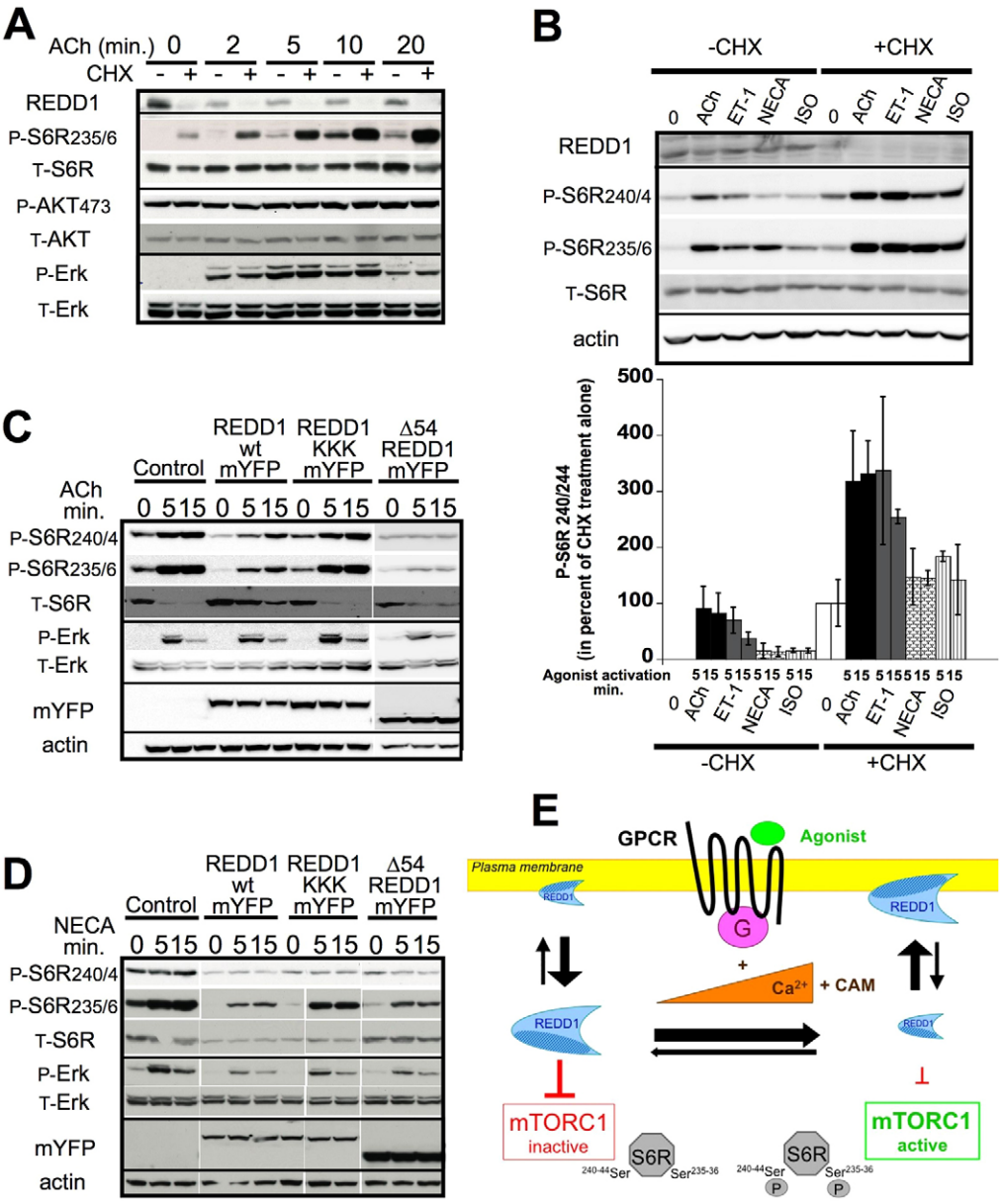

Fig. 8. REDD1 control of mTORC1 in HEK293 cells. (A) Rapid degradation of REDD1 releases the TSC1/2 brake on mTORC1 activity. Western blots using 20 μg of HEK293 cell protein extracts after overnight serum starvation, 12-minute CHX (50 μM) treatment and ACh activation up to 20 minutes. Representative data, $n=3$. (B) GPCR agonists activate mTORC1 in the absence of REDD1. Top panel, representative western blots using 20 μg of HEK293 cell protein extracts after overnight serum starvation, 12 minutes of CHX (50 μM) treatment and agonist activation for 5 minutes. Bottom panel, quantification of P-S6R in percentage of CHX treatment alone after 5 or 15 minute activation with agonists ($n=2$; means ± s.d.). Functional overexpressed REDD1 reduces mTORC1 activity upon stimulation with Gq-coupled M3R (C) or Gs-coupled Ade2BR (D). Western blots using extracts from control untransfected cells or stable cell lines overexpressing REDD1wt–mYFP, REDD1-KKK–mYFP or Δ54-REDD1–mYFP. Representative data, $n=2$. (E) Model of the GPCR/REDD1/mTORC1 pathway.

In conclusion, the basal level of REDD1 most likely has an inhibitory effect on mTORC1 (as already proposed in previous studies), whereas overexpressed REDD1 reduces the activity of mTORC1 regulated by GPCRs. There is a correlation between fast and robust REDD1 translocation to the plasma membrane and fast mTORC1 activation by GPCRs. In addition, the mTORC1-inhibitory motif is required for plasma membrane localization and translocation. Thus, translocation to the plasma membrane seems to be a mechanism of inactivation of REDD1 by GPCRs probably by sequestering the mTORC1-inhibitory motif in the membrane (Fig. 8E).

DISCUSSION

In the present study, we have used a live-imaging screen to identify new cytoplasmic proteins that participate in the on and off cycle of GPCRs based on spatio-temporal criteria. Our data demonstrate that REDD1, identified during the screen, is a novel general effector of GPCRs because it is specifically translocated to the plasma membrane in response to activation of five out of six endogenously expressed GPCRs that were tested, namely, those that couple preferentially to Gq, Gs or Gi heterotrimeric G-proteins, but not to G12.

Regulation of the plasma membrane translocation of REDD1

Our study establishes that a fraction of REDD1 is localized at the plasma membrane and that this localization is regulated. Differences in the kinetics and amplitudes of plasma membrane translocation of REDD1 were clearly observed. Both Gq-coupled receptors gave a similar translocation profile, that was fast and had a large amplitude. The two Gs-coupled receptors tested can also be grouped in terms of profile of REDD1 translocation: slower translocation and an intermediate amplitude. Gi-coupled CXCR4 gave the smallest amplitude of REDD1 translocation. These differences in kinetics and amplitudes were not correlated

Journal of Cell Science (2014) 127, 773–787 doi:10.1242/jcs.136432

with the receptor expression levels described in the literature (supplementary material Table S1). Instead, we found a correlation with the amplitude of the intracellular increase in Ca^{2+} generated upon activation of each GPCR. A Ca^{2+} rise independent of GPCR activation was not sufficient to translocate REDD1 to the plasma membrane, but calcium and calmodulin were found necessary. In addition, the observation that most of the tested GPCRs can translocate REDD1 indicates that this involves a common GPCR signaling pathway.

Although some GPCRs can couple to several types of heterotrimeric G proteins (Hermans, 2003), we do not favor the hypothesis that the Ca^{2+} increase induced by the tested GPCRs could be the result of coupling to Gq. Endogenously expressed Gi-coupled receptors have been shown to increase the intracellular Ca^{2+}concentration through activation of Gβγ, Gs-coupled Beta-2adrR mediates Ca^{2+} responses through activation of Ca^{2+} channels and G12-coupled receptors through activation of Rho and PLCε (phospholipase C epsilon) (supplementary material Table S1). In addition, coupling to multiple G-proteins might be more pronounced if the receptors are overexpressed and could depend upon the degree of biased agonism of the tested ligand (Galandrin et al., 2007). Instead, in our study, receptors were endogenously expressed and all the agonists were either the natural endogenous agonists (ACh, ET-1, CXCL12, LPA) or behave like natural agonists in terms of ligand signaling profile (Iso) (Stallaert et al., 2012) with one exception, NECA, that might induce Gq-coupling to Ade2BR (Gao et al., 1999).

Based on the translocation kinetics of the REDD1-KY mutant triggered by Gq-coupled receptors, which is transient, it seems that the mechanism of REDD1 translocation to the plasma membrane can be decomposed into at least two phases: the translocation itself (cytosol to plasma membrane) dependent on heterotrimeric G activation, calcium and calmodulin, and the membrane tethering of REDD1. On the basis of the profile of the translocation kinetics of this same mutant, REDD1-KY, triggered by Gs-coupled receptors (kinetics and amplitudes identical to REDD1wt), we propose that the membrane tethering of REDD1 can be mediated by different components depending on the signaling cascades.

Three lines of evidence support the hypothesis that the lipid composition of the inner leaflet of the membrane plays a role in REDD1 tethering at the plasma membrane: first, the strong plasma membrane BRET signal detected with REDD1 in resting cells suggests a close proximity with the lipid bilayer. Second, the stretch of positively charged lysine residues necessary for plasma membrane association of REDD1 could constitute a binding motif to the negatively charged phospholipids of the plasma membrane (Heo et al., 2006). Third, activation of GPCRs is known to modify the lipid composition of the inner leaflet of the plasma membrane (An et al., 2011).

Our data show that the REDD1 homolog REDD2 is neither located at the plasma membrane in resting cells nor does it respond to GPCR activation. We have demonstrated that at least two domains contribute to membrane localization and translocation of REDD1: its Nt extension, absent in REDD2, and the mTORC1-inhibitory motif, which is conserved in REDD2.

The importance of the REDD1 Nt domain

Little is known about the Nt of REDD1. For the determination of the 3D structure, this flexible domain had to be deleted in order to obtain crystals (Vega Rubin de Celis et al., 2010). Our data clearly establish that the unique Nt of REDD1 can trigger both association of REDD2 with membranes, including the plasma membrane, and regulation of REDD2 translocation by GPCR signaling. Thus, the Nt extension of REDD1 is an important regulatory domain and we hypothesize that it contributes to a conformational rearrangement of REDD1 upon GPCR–Ca^{2+}/calmodulin activation, which displaces the equilibrium towards a conformation of REDD1 that has more affinity for the membrane. Of note, there was no detectable translocation of an N-terminally tagged REDD1 upon NK2R activation in the original screening, suggesting an interference of the fluorophore on the proper folding of the Nt extension of REDD1. Solving the structure of the entire protein and analysing the dynamic aspect of the regulation using biophysical approaches, such as environment sensitive-probes would certainly help in understanding the function of REDD1 at the molecular level.

Competitive interactions at the level of the mTORC1-inhibitory motif

Several findings suggest that the mTORC1-inhibitory motif is the site for competitive interactions with different molecules. The stretch of lysine residues 218 to 220 serves as a targeting signal of REDD1 to the mitochondria (Horak et al., 2010, mutations K218S/K219S/K220S). Here, we show that the same residues target REDD1 to the plasma membrane (mutations K218A/K219A/K220A). In addition, we demonstrated that this REDD1-KKK mutant is altered in its capacity to inhibit mTORC1 function. Although controversy remains as to which molecular partner associates with REDD1 when activating the TSC1/2 complex [e.g. the 14-3-3 proteins (DeYoung et al., 2008, Morrison, 2009), the TSC2 protein (Quarcks Inc.) or an unidentified molecule], our data suggest that GPCRs are sequestering this mTORC1-inhibitory motif into the plasma membrane, away from its site of action on the mTORC1 pathway.

A novel mechanism of action of GPCRs on mTORC1 function

mTORC1 integrates inputs from multiple signaling pathways, including growth factors and mitogens. mTORC1 also functions as a sensor of cellular nutrients, energy level and redox status. There are reports showing that mTORC1 can be activated by GPCRs, but it is not yet recognized as a canonical pathway (Musnier et al., 2010; del Toro et al., 2010; Wauson et al., 2012; Varghese et al., 2013). Three mechanisms of activation have been described: modulation of mTORC1 via transactivation of RTK/PI3K/AKT by GPCRs and/or by MAP-kinase (Raf/MEK/ERK) signaling (Rozengurt 2007) and more recently, a direct interaction was discovered between the serotonin 5-HT(6) receptor and many proteins from the mTORC1 pathway, including the mTOR kinase itself (Meffre et al., 2012).

Our study places the mTORC1 pathway as a downstream target of GPCR signaling through a novel link, the REDD1 protein. Because mTORC1 is a classical target for receptor tyrosine kinases, it suggests another level of crosstalk between RTK and GPCR signaling networks, via REDD1, which would benefit from being explored in pathological, as well as physiological cellular contexts. For example, the interesting role of the diabetes drug metformin in the inhibition of the crosstalk between insulin receptors and GPCRs in pancreatic cancer cells (Rozengurt et al., 2010) could be linked to REDD1 expression as shown in prostate cancer cells (Ben Sahra et al., 2011). The question of crosstalk between GPCRs, REDD1 and RTKs is complicated owing to possible negative-feedback controls: for example, REDD1 is induced by insulin in skeletal muscles (Frost et al., 2009) and in adipocytes (Regazzetti et al., 2010), where REDD1 positively

Journal of Cell Science (2014) 127, 773–787 doi:10.1242/jcs.136432

regulates insulin signaling through the inhibition of mTORC1 activity that exerts a negative-feedback control on insulin signaling (Regazzetti et al., 2012).

The Gq-coupled GPCRs that we have tested, and to a lesser extent the Gs-coupled ones, activate mTORC1 in the absence of REDD1, suggesting that GPCRs have a positive input at several protein levels in the mTORC1 pathway and not only at the level of REDD1. The mTORC1 pathway controls cell size, and together with the recent demonstration that GPCRs can also regulate the Hippo-YAP pathway that controls cell number (Yu et al., 2012), this might have broad implications in terms of organ size control and tumorogenesis (Tumaneng et al., 2012). Phosphorylation of YAP was found to be maximal with activation of G12-coupled GPCRs but intermediate with activation of Gq- or Gi-coupled GPCRs. Inversely, phosphorylation of YAP was found to be inhibited by Gs-coupled GPCRs (Yu et al., 2012). Interestingly, we have found a different G-coupling ranking for REDD1 translocation by the tested GPCRs: maximal with Gq, intermediate with Gs, low with Gi and absent with G12.

Roles for basal levels of REDD1 expression

REDD1 has been shown to contribute to suppression of tumorogenesis through its inhibition of mTORC1 (Ben Sahra et al., 2011). It is a host defence factor against RNA viruses (Mata et al., 2011). It is implicated in neurogenesis and neurodegenerative diseases (Malagelada et al., 2011) and controls Schwann cell myelination in mice (Noseda et al., 2013). Its orthologs in *Drosophila* and Zebrafish participate in development (Scuderi et al., 2006, Feng et al., 2012). With our demonstration of a basal level of REDD1 localized at the plasma membrane, it would be interesting to develop specific inhibitors against REDD1 localization and/or translocation to the plasma membrane to further dissect the role of REDD1 in this cell compartment and refine our understanding of physiological responses to cellular stresses.

MATERIALS AND METHODS

Ligands

EGF was obtained from Bachem; insulin, acetylcholine chloride, AMD3100 and atropin sulfate were from Sigma-Aldrich; isoproterenol hydrochloride, alprenolol, NECA, CGS15943, endothelin-1 and sulfisoxazole were from Tocris; LPA was obtained from Avanti Polar lipids (Coger); CXCL12 was purified in the laboratory (Hachet-Haas et al., 2008).

Inhibitors

Several inhibitors were also used: CoCl2 (Sigma), cycloheximide (Tocris), W7 (Calbiochem), BAPTA-AM (Enzo Life science).

Antibodies

HRP-goat anti-rabbit was from Jackson Immunoresearch; HRP-goat anti-mouse from GE-Healthcare; and rabbit polyclonal anti-phospho-S6R (Ser240/244) dilution 1:6000, anti-phospho-S6R (Ser235/236) dilution 1:6000 were from Cell Signaling; antibodies against P-ERK (Thr185/Tyr187) dilution 1:5000 were from Invitrogen and total ERK (dilution 1:10,000) were from Enzo Life Science. Rabbit monoclonal anti-phospho-p70S6K (Thr389) (dilution 1:10,000), antibody against total p70S6K (dilution 1:10,000), anti-P-AKT (Ser473) (dilution 1:20,000) and anti-P-AKT (Thr308) (dilution 1:2000) were from Epitomics, Euromedex. Mouse monoclonal antibody against total S6R (dilution 1:2000) was from Cell Signaling, Ozyme and anti-actin clone C4 (1:100,000) was from Merck-Millipore.

Cell culture

All cell lines were based on HEK293 cells, and clonal cell lines stably expressing human NK2R, Myr-Palm–mYFP, YFP–actin, Gbeta–YFP, REDD1wt–mYFP or REDD1mutant–mYFP were cultivated as previously described (Hachet-Haas et al., 2006).

Live-imaging screening by microscopy

HEK293 cells expressing the non-fluorescent NK2R were plated into four eight-well Labtek chambers with glass-slides (Nunc). 150 ng of individual vectors were transiently transfected using the calcium phosphate technique. Each fluorescent protein was observed after 24 hours of expression under the spinning-disk ultraview confocal microscope (Perkin Elmer) equipped with an incubation box allowing maintenance at 37℃ using the 63× objective. The field to be filmed (displaying around five cells) was chosen manually by assessing the fluorescent expression of each clone, cells were chosen for detectable but low and homogenous expression of the fluorescence. One video of 90 seconds recorded the activation process: the focus was placed in the z-axis in the middle of the cell; activation with 100 nM NKA [in buffer HEPES-BSA: 137.5 mM NaCl, 1.25 mM MgCl2, 1.25 mM $CaCl_2$, 6 mM KCl, 5.6 mM glucose,10 mM HEPES, 0.4 mM NaH_2PO_4, 0.1% BSA (w/v), pH 7.4] was performed after 20 seconds recording while filming was in progress, allowing the visualization of the fluorescent protein before activation and its eventual short-term translocation upon induction (usually and depending on the expression level of the fluorescent protein tested, the exposure-time was between 399 and 999 milliseconds with Binning 1 for YFP samples and Binning 4 for CFP samples). Videos were generated using ImageJ software. Two subsequent videos of 15 seconds were recorded around 1 hour and 4 hours after activation.

4D live imaging

Image acquisition and deconvolutions were performed as previously described (Savino et al., 2001; De Mey et al., 2008).

Creating generic expression vectors with the LIC system

The REDD1 fragment was generated by PCR and subcloned into pcDNA3 by inserting a *Kpn*I-REDD1-*Not*I PCR fragment using pd-humanREDD1-EYFP as a template (Simpson et al., 2000). pCMV6-XL5-human REDD2 and AKT1 were purchased at OriGene (number SC100121, NM_145244; SC16883, NM_005163, respectively. (NtRedd1)-REDD2 was subcloned by the overlap extension PCR cloning method (Bryksin and Matsumura, 2010). The REDD1 mutants were first created in pcDNA3 using the QuikChange mutagenesis kit from Stratagene using pcDNA3-REDD1 vector as a bait (supplementary material Table S2). Expression vectors for fusion proteins containing either the mYFP fluorophore or the RLuc luciferase or its RLuc8 mutant were generated with the LIC method as described (Hachet-Haas et al., 2006). The protein X of interest is separated from the mYFP or the RLuc by a six-residue linker, LeuSerAsnGluAsnGlu.

Confocal fluorescent microscopy

Cells were plated in 24-well plates on 12 mm glass coverslips. Cells were rinsed in warm PHEM buffer (60 mM PIPES, 25 mM HEPES, 10 mM EGTA and 2 mM $MgCl_2$) then fixed for 12 minutes. in 4% paraformaldehyde and 0.05% glutaraldehyde with 0.05% Triton X-100 in 1× PHEM. Coverslips were rinsed with PBS, then incubated twice for 10 minutes in 1 mg/ml $NaBH_4$. Actin was detected by a 15 minute staining with 1 Unit Texas-Red–X-Phalloidin (Molecular Probes, Invitrogen). Coverslips were mounted onto microscope slides using Mowiol antifading agent (Calbiochem). Image acquisition was performed as described (Hachet-Haas et al., 2006), with an inverted microscope (Leica) and a laser-scanning confocal imaging system (SP2-UV or AOBS SP2 RS) using a HCX PL APO CS 100× 1.40 oil immersion UV objective. To obtain a good signal-to-noise ratio, the images were averages from eight consecutive acquisitions.

BRET1 assays

Cells were seeded in six-well plates and transfected with Lipofectamine 2000 for 48 hours. For end-point kinetic experiments or real-time well-to-well kinetics, cells were treated as described previously (Ouedraogo et al. 2008). BRET1 signal was counted at 37℃ in a

VictorLight apparatus (Perkin Elmer) at 3 mm from the bottom of the plate. Two consecutive signals were registered over 1 second each: luminescent signal (band-pass filter 435–485 nm, 'donor RLuc channel') then the energy transfer signal (band-pass filter 510–560 nm, 'acceptor YFP channel'). For end-point kinetics, measures were performed with 5 µM coelenterazine H (Molecular Probes). For real-time well-to-well kinetics, cells were incubated with 60 µM of Enduren (Promega) diluted in HEPES-BSA buffer for 2 hours before starting the recordings. BRET1 signal was then registered usually in two or four consecutives wells before vehicle or ligand activation for 10 minutes. BRET1 signals were continuously recorded after treatment for up to 30 minutes.

BRET1 equations are the following: 'BRET ratio' = [signal in cps (counts per second) counted in the acceptor YFP channel] / (signal in the donor RLuc channel). 'net BRET' = (BRET ratio of cells expressing both RLuc and YFP fusion proteins) – (BRET ratio of cells expressing only RLuc fusion protein). The 'drug induced BRET' = (BRET ratio with the drug) – (BRET ratio without drug).

For all the experiments with the mutants of REDD and for comparative purposes, when setting up the BRET experiments, the relative expression levels of tagged proteins were controlled by measuring the luminescent signal. The amount of DNA that encodes proteins to be compared for transient transfection was accordingly modified in order to have similar expression levels. To limit overexpression, luminescent signals were also adjusted to be the closest to the minimal luminescent intensity necessary for a reproducible BRET signal to be detected with the Victor-Light apparatus.

Biochemical membrane fractionation

Cells cultivated in six-well plates for 2 days were dissociated from the dishes in pre-warmed PBS with 5 mM EDTA. Cells were collected by centrifugation at 2000 ***g*** at 4℃ and resuspended in 200 µl of lysis buffer [10 mM Tris-HCl, pH 7.5, 150 mM NaCl, 1 mM DTT, complete-EDTA free, anti-protease and anti-phosphatase cocktails (Roche)]. They were lysed at 4℃ by passing 100 times through a 22 G needle on a 1 ml syringe. A post-nuclear supernatant (PNS) was obtained by centrifuging the lysates for 10 minutes at 2000 ***g*** at 4℃. The PNS was centrifuged at 100,000 ***g*** for 30 minutes using a TLA-100.3 rotor. Pellets (P) were resuspended in a 1:1 lysis buffer, 2× Laemmli mix and supernatant (S) in 2× Laemmli buffer.

Signaling assays

Ca^{2+} responses were measured as described previously (Hachet-Haas et al., 2008). For mTORC1 kinase activation assays, cells were seeded in six-well plates (350,000 cells/well), serum starved overnight before activation with agonists and/or inhibitors for different times at 37℃. The stimulation was terminated by discarding the medium and lysing the cells in 250 µl of cold RIPA buffer (50 mM Tris-HCl, pH 7.4, 150 mM NaCl, 1% NP40, 0.25% sodium deoxycholate) supplemented with EDTA-free anti-protease and anti-phosphatase cocktails. For western blotting, the immunoreactive bands were visualized using Immobilon Western chemoluminescent HRP substrate detection reagents (Merck-Millipore) either with hyperfilm or LAS 4000 camera, bands were quantified using ImageQuant software (GE-Healthcare).

Acknowledgements

pcDNA3-myristoylated-palmitoylated-mYFP was from R. Tsien, pRLuc8 from S.S. Gambhir, pC3-pEYFP-Actin from F.C. Nielsen (University of Copenhagen, Denmark). We are grateful to all members of UMS3286 and of the facilities at IGBMC, including J.L. Plassat for quantitative RT-PCR. Many thanks to E. Pencreach, Inserm U682, N. Larbi, and all M. Bouvier's lab members in IRIC, in particular P. René and B. Breton for help setting up mTORC1, AKT translocation and BRET assays, respectively. We thank members of the Galzi–Simonin lab, particularly R. Wagner and B. Ilien for support, V. Utard for maintenance of the cell culture facility and J. Garwood for critical reading of the manuscript.

Competing interests

The authors declare that they have no conflicts of interest.

Author contributions

G.M. performed BRET, Ca^{2+} and mTORC1 assays; H.W.D.M. did cloning and mutagenesesis experiments and designed the REDD1 polyclonal antibodies preparation; M.H.H. performed Ca^{2+} and mTORC1 assays, purified CXCL12 and participated in the writing of the manuscript; K.E.B. participated in setting up of the BRET assays; J.d.M. did the acquisition and analysis of 4D-videos; R.P. participated in the design of the live-imaging screen; J.C.S. shared his knowlegde in the design and performance of the live-imaging screen and in the writing of the manuscript; J.L.G. participated in the design and follow-up of the project, and in the writing of the manuscript; S.L. designed and coordinated the project and the experiments, performed research experiments, analyzed the results, prepared the figures and wrote the manuscript.

Funding

This work was supported by the French Ministry of Research (BCMS grant and PhD contract for G.M.), EMBO, and a HFSP short-term fellowships to S.L.

Supplementary material

Supplementary material available online at
http://jcs.biologists.org/lookup/suppl/doi:10.1242/jcs.136432/-/DC1

References

An, S. W., Cha, S. K., Yoon, J., Chang, S., Ross, E. M. and Huang, C. L. (2011). WNK1 promotes PIP_2 synthesis to coordinate growth factor and GPCR-Gq signaling. *Curr. Biol.* **21**, 1979-1987.

Atwood, B. K., Lopez, J., Wager-Miller, J., Mackie, K. and Straiker, A. (2011). Expression of G protein-coupled receptors and related proteins in HEK293, AtT20, BV2, and N18 cell lines as revealed by microarray analysis. *BMC Genomics* **12**, 14.

Ben Sahra, I., Regazzetti, C., Robert, G., Laurent, K., Le Marchand-Brustel, Y., Auberger, P., Tanti, J. F., Giorgetti-Peraldi, S. and Bost, F. (2011). Metformin, independent of AMPK, induces mTOR inhibition and cell-cycle arrest through REDD1. *Cancer Res.* **71**, 4366-4372.

Benitah, J. P., Alvarez, J. L. and Gómez, A. M. (2010). L-type Ca(2+) current in ventricular cardiomyocytes. *J. Mol. Cell Cardiol.* **48**, 26-36.

Brugarolas, J., Lei, K., Hurley, R. L., Manning, B. D., Reiling, J. H., Hafen, E., Witters, L. A., Ellisen, L. W. and Kaelin, W. G., Jr (2004). Regulation of mTOR function in response to hypoxia by REDD1 and the TSC1/TSC2 tumor suppressor complex. *Genes Dev.* **18**, 2893-2904.

Bryksin, A. V. and Matsumura, I. (2010). Overlap extension PCR cloning: a simple and reliable way to create recombinant plasmids. *Biotechniques* **48**, 463-465.

Busillo, J. M., Armando, S., Sengupta, R., Meucci, O., Bouvier, M. and Benovic, J. L. (2010). Site-specific phosphorylation of CXCR4 is dynamically regulated by multiple kinases and results in differential modulation of CXCR4 signaling. *J. Biol. Chem.* **285**, 7805-7817.

Cézanne, L., Lecat, S., Lagane, B., Millot, C., Vollmer, J. Y., Matthes, H., Galzi, J. L. and Lopez, A. (2004). Dynamic confinement of NK2 receptors in the plasma membrane. Improved FRAP analysis and biological relevance. *J. Biol. Chem.* **279**, 45057-45067.

Corradetti, M. N., Inoki, K. and Guan, K. L. (2005). The stress-inducted proteins RTP801 and RTP801L are negative regulators of the mammalian target of rapamycin pathway. *J. Biol. Chem.* **280**, 9769-9772.

Daulat, A. M., Maurice, P. and Jockers, R. (2009). Recent methodological advances in the discovery of GPCR-associated protein complexes. *Trends Pharmacol. Sci.* **30**, 72-78.

De Mey, J. R., Kessler, P., Dompierre, J., Cordelières, F. P., Dieterlen, A., Vonesch, J. L. and Sibarita, J. B. (2008). Fast 4D Microscopy. *Methods Cell Biol.* **85**, 83-112.

del Toro, R., Prahst, C., Mathivet, T., Siegfried, G., Kaminker, J. S., Larrivee, B., Breant, C., Duarte, A., Takakura, N., Fukamizu, A. et al. (2010). Identification and functional analysis of endothelial tip cell-enriched genes. *Blood* **116**, 4025-4033.

DeYoung, M. P., Horak, P., Sofer, A., Sgroi, D. and Ellisen, L. W. (2008). Hypoxia regulates TSC1/2-mTOR signaling and tumor suppression through REDD1-mediated 14-3-3 shuttling. *Genes Dev.* **22**, 239-251.

Drake, M. T., Violin, J. D., Whalen, E. J., Wisler, J. W., Shenoy, S. K. and Lefkowitz, R. J. (2008). beta-arrestin-biased agonism at the beta2-adrenergic receptor. *J. Biol. Chem.* **283**, 5669-5676.

Edwards, D. R. (1994). Cell signalling and the control of gene transcription. *Trends Pharmacol. Sci.* **15**, 239-244.

Ellisen, L. W. (2005). Growth control under stress: mTOR regulation through the REDD1-TSC pathway. *Cell Cycle* **4**, 1500-1502.

Ellisen, L. W., Ramsayer, K. D., Johannessen, C. M., Yang, A., Beppu, H., Minda, K., Oliner, J. D., McKeon, F. and Haber, D. A. (2002). REDD1, a developmentally regulated transcriptional target of p63 and p53, links p63 to regulation of reactive oxygen species. *Mol. Cell* **10**, 995-1005.

Feng, Q., Zou, X., Lu, L., Li, Y., Liu, Y., Zhou, J. and Duan, C. (2012). The stress-response gene redd1 regulates dorsoventral patterning by antagonizing Wnt/β-catenin activity in zebrafish. *PLoS ONE* **7**, e52674.

Franke, T. F., Kaplan, D. R., Cantley, L. C. and Toker, A. (1997). Direct regulation of the Akt proto-oncogene product by phosphatidylinositol-3,4-bisphosphate. *Science* **275**, 665-668.

Friedman, J., Babu, B. and Clark, R. B. (2002). Beta(2)-adrenergic receptor lacking the cyclic AMP-dependent protein kinase consensus sites fully activates extracellular signal-regulated kinase 1/2 in human embryonic kidney 293 cells: lack of evidence for G(s)/G(i) switching. *Mol. Pharmacol.* **62**, 1094-1102.

Frost, R. A., Huber, D., Pruznak, A. and Lang, C. H. (2009). Regulation of REDD1 by insulin-like growth factor-I in skeletal muscle and myotubes. *J. Cell. Biochem.* **108**, 1192-1202.
Galandrin, S., Oligny-Longpré, G. and Bouvier, M. (2007). The evasive nature of drug efficacy: implications for drug discovery. *Trends Pharmacol. Sci.* **28**, 423-430.
Gao, Z., Chen, T., Weber, M. J. and Linden, J. (1999). A2B adenosine and P2Y2 receptors stimulate mitogen-activated protein kinase in human embryonic kidney-293 cells. cross-talk between cyclic AMP and protein kinase c pathways. *J. Biol. Chem.* **274**, 5972-5980.
Gicquiaux, H., Lecat, S., Gaire, M., Dieterlen, A., Mély, Y., Takeda, K., Bucher, B. and Galzi, J. L. (2002). Rapid internalization and recycling of the human neuropeptide Y Y(1) receptor. *J. Biol. Chem.* **277**, 6645-6655.
Hachet-Haas, M., Converset, N., Marchal, O., Matthes, H., Gioria, S., Galzi, J. L. and Lecat, S. (2006). FRET and colocalization analyzer—a method to validate measurements of sensitized emission FRET acquired by confocal microscopy and available as an ImageJ Plug-in. *Microsc. Res. Tech.* **69**, 941-956.
Hachet-Haas, M., Balabanian, K., Rohmer, F., Pons, F., Franchet, C., Lecat, S., Chow, K. Y., Dagher, R., Gizzi, P., Didier, B. et al. (2008). Small neutralizing molecules to inhibit actions of the chemokine CXCL12. *J. Biol. Chem.* **283**, 23189-23199.
Hains, M. D., Wing, M. R., Maddileti, S., Siderovski, D. P. and Harden, T. K. (2006). Galpha12/13- and rho-dependent activation of phospholipase C-epsilon by lysophosphatidic acid and thrombin receptors. *Mol. Pharmacol.* **69**, 2068-2075.
Haribabu, B., Richardson, R. M., Fisher, I., Sozzani, S., Peiper, S. C., Horuk, R., Ali, H. and Snyderman, R. (1997). Regulation of human chemokine receptors CXCR4. Role of phosphorylation in desensitization and internalization. *J. Biol. Chem.* **272**, 28726-28731.
Heo, W. D., Inoue, T., Park, W. S., Kim, M. L., Park, B. O., Wandless, T. J. and Meyer, T. (2006). PI(3,4,5)P3 and PI(4,5)P2 lipids target proteins with polybasic clusters to the plasma membrane. *Science* **314**, 1458-1461.
Hermans, E. (2003). Biochemical and pharmacological control of the multiplicity of coupling at G-protein-coupled receptors. *Pharmacol. Ther.* **99**, 25-44.
Horak, P., Crawford, A. R., Vadysirisack, D. D., Nash, Z. M., DeYoung, M. P., Sgroi, D. and Ellisen, L. W. (2010). Negative feedback control of HIF-1 through REDD1-regulated ROS suppresses tumorigenesis. *Proc. Natl. Acad. Sci. USA* **107**, 4675-4680.
Hudson, C. C., Oakley, R. H., Sjaastad, M. D. and Loomis, C. R. (2006). High-content screening of known G protein-coupled receptors by arrestin translocation. *Methods Enzymol.* **414**, 63-78.
Inoki, K., Li, Y., Zhu, T., Wu, J. and Guan, K. L. (2002). TSC2 is phosphorylated and inhibited by Akt and suppresses mTOR signalling. *Nat. Cell Biol.* **4**, 648-657.
Jiang, H., Kuang, Y., Wu, Y., Smrcka, A., Simon, M. I. and Wu, D. (1996). Pertussis toxin-sensitive activation of phospholipase C by the C5a and fMet-Leu-Phe receptors. *J. Biol. Chem.* **271**, 13430-13434.
Katiyar, S., Liu, E., Knutzen, C. A., Lang, E. S., Lombardo, C. R., Sankar, S., Toth, J. I., Petroski, M. D., Ronai, Z. and Chiang, G. G. (2009). REDD1, an inhibitor of mTOR signalling, is regulated by the CUL4A-DDB1 ubiquitin ligase. *EMBO Rep.* **10**, 866-872.
Kimball, S. R., Do, A. N., Kutzler, L., Cavener, D. R. and Jefferson, L. S. (2008). Rapid turnover of the mTOR complex 1 (mTORC1) repressor REDD1 and activation of mTORC1 signaling following inhibition of protein synthesis. *J. Biol. Chem.* **283**, 3465-3475.
Lecat, S., Ouédraogo, M., Cherrier, T., Noulet, F., Rondé, P., Glasser, N., Galzi, J. L., Mely, Y., Takeda, K. and Bucher, B. (2011). Contribution of a tyrosine-based motif to cellular trafficking of wild-type and truncated NPY Y(1) receptors. *Cell. Signal.* **23**, 228-238.
Lin, L., Stringfield, T. M., Shi, X. and Chen, Y. (2005). Arsenite induces a cell stress-response gene, RTP801, through reactive oxygen species and transcription factors Elk-1 and CCAAT/enhancer-binding protein. *Biochem. J.* **392**, 93-102.
Linden, J., Thai, T., Figler, H., Jin, X. and Robeva, A. S. (1999). Characterization of human A(2B) adenosine receptors: radioligand binding, western blotting, and coupling to G(q) in human embryonic kidney 293 cells and HMC-1 mast cells. *Mol. Pharmacol.* **56**, 705-713.
Loening, A. M., Fenn, T. D., Wu, A. M. and Gambhir, S. S. (2006). Consensus guided mutagenesis of Renilla luciferase yields enhanced stability and light output. *Protein Eng. Des. Sel.* **19**, 391-400.
Malagelada, C., López-Toledano, M. A., Willett, R. T., Jin, Z. H., Shelanski, M. L. and Greene, L. A. (2011). RTP801/REDD1 regulates the timing of cortical neurogenesis and neuron migration. *J. Neurosci.* **31**, 3186-3196.
Mata, M. A., Satterly, N., Versteeg, G. A., Frantz, D., Wei, S., Williams, N., Schmolke, M., Peña-Llopis, S., Brugarolas, J., Forst, C. V. et al. (2011). Chemical inhibition of RNA viruses reveals REDD1 as a host defense factor. *Nat. Chem. Biol.* **7**, 712-719.
Meffre, J., Chaumont-Dubel, S., Mannoury la Cour, C., Loiseau, F., Watson, D. J., Dekeyne, A., Séveno, M., Rivet, J. M., Gaven, F., Déléris, P. et al. (2012). 5-HT(6) receptor recruitment of mTOR as a mechanism for perturbed cognition in schizophrenia. *EMBO Mol. Med.* **4**, 1043-1056.
Miyazaki, M. and Esser, K. A. (2009). REDD2 is enriched in skeletal muscle and inhibits mTOR signaling in response to leucine and stretch. *Am. J. Physiol.* **296**, C583-C592.
Montmayeur, J. P., Barr, T. P., Kam, S. A., Packer, S. J. and Strichartz, G. R. (2011). ET-1 induced Elevation of intracellular calcium in clonal neuronal and embryonic kidney cells involves endogenous endothelin-A receptors linked to phospholipase C through Gα(q/11). *Pharmacol. Res.* **64**, 258-267.
Morrison, D. K. (2009). The 14-3-3 proteins: integrators of diverse signaling cues that impact cell fate and cancer development. *Trends Cell Biol.* **19**, 16-23.
Musnier, A., Blanchot, B., Reiter, E. and Crépieux, P. (2010). GPCR signalling to the translation machinery. *Cell. Signal.* **22**, 707-716.
Noseda, R., Belin, S., Piguet, F., Vaccari, I., Scarlino, S., Brambilla, P., Martinelli Boneschi, F., Feltri, M. L., Wrabetz, L., Quattrini, A. et al. (2013). DDIT4/REDD1/RTP801 is a novel negative regulator of Schwann cell myelination. *J. Neurosci.* **33**, 15295-15305.
Ouedraogo, M., Lecat, S., Rochdi, M. D., Hachet-Haas, M., Matthes, H., Gicquiaux, H., Verrier, S., Gaire, M., Glasser, N., Mély, Y. et al. (2008). Distinct motifs of neuropeptide Y receptors differentially regulate trafficking and desensitization. *Traffic* **9**, 305-324.
Regazzetti, C., Bost, F., Le Marchand-Brustel, Y., Tanti, J. F. and Giorgetti-Peraldi, S. (2010). Insulin induces REDD1 expression through hypoxia-inducible factor 1 activation in adipocytes. *J. Biol. Chem.* **285**, 5157-5164.
Regazzetti, C., Dumas, K., Le Marchand-Brustel, Y., Peraldi, P., Tanti, J. F. and Giorgetti-Peraldi, S. (2012). Regulated in development and DNA damage responses −1 (REDD1) protein contributes to insulin signaling pathway in adipocytes. *PLoS ONE* **7**, e52154.
Reiling, J. H. and Hafen, E. (2004). The hypoxia-induced paralogs Scylla and Charybdis inhibit growth by down-regulating S6K activity upstream of TSC in Drosophila. *Genes Dev.* **18**, 2879-2892.
Roux, P. P., Shahbazian, D., Vu, H., Holz, M. K., Cohen, M. S., Taunton, J., Sonenberg, N. and Blenis, J. (2007). RAS/ERK signaling promotes site-specific ribosomal protein S6 phosphorylation via RSK and stimulates cap-dependent translation. *J. Biol. Chem.* **282**, 14056-14064.
Rozengurt, E. (2007). Mitogenic signaling pathways induced by G protein-coupled receptors. *J. Cell. Physiol.* **213**, 589-602.
Rozengurt, E., Sinnett-Smith, J. and Kisfalvi, K. (2010). Crosstalk between insulin/insulin-like growth factor-1 receptors and G protein-coupled receptor signaling systems: a novel target for the antidiabetic drug metformin in pancreatic cancer. *Clin. Cancer Res.* **16**, 2505-2511.
Savino, T. M., Gébrane-Younès, J., De Mey, J., Sibarita, J. B. and Hernandez-Verdun, D. (2001). Nucleolar assembly of the rRNA processing machinery in living cells. *J. Cell Biol.* **153**, 1097-1110.
Schwarzer, R., Tondera, D., Arnold, W., Giese, K., Klippel, A. and Kaufmann, J. (2005). REDD1 integrates hypoxia-mediated survival signaling downstream of phosphatidylinositol 3-kinase. *Oncogene* **24**, 1138-1149.
Scuderi, A., Simin, K., Kazuko, S. G., Metherall, J. E. and Letsou, A. (2006). scylla and charybde, homologues of the human apoptotic gene RTP801, are required for head involution in Drosophila. *Dev. Biol.* **291**, 110-122.
Shaw, G., Morse, S., Ararat, M. and Graham, F. L. (2002). Preferential transformation of human neuronal cells by human adenoviruses and the origin of HEK 293 cells. *FASEB J.* **16**, 869-871.
Shenoy, S. K., Drake, M. T., Nelson, C. D., Houtz, D. A., Xiao, K., Madabushi, S., Reiter, E., Premont, R. T., Lichtarge, O. and Lefkowitz, R. J. (2006). beta-arrestin-dependent, G protein-independent ERK1/2 activation by the beta2 adrenergic receptor. *J. Biol. Chem.* **281**, 1261-1273.
Shoshani, T., Faerman, A., Mett, I., Zelin, E., Tenne, T., Gorodin, S., Moshel, Y., Elbaz, S. M., Budanov, A., Chajut, A. et al. (2002). Identification of a novel hypoxia-inducible factor 1-responsive gene, RTP801, involved in apoptosis. *Mol. Cell Biol.* **7**, 2283-2293.
Simpson, J. C., Wellenreuther, R., Poustka, A., Pepperkok, R. and Wiemann, S. (2000). Systematic subcellular localization of novel proteins identified by large-scale cDNA sequencing. *EMBO Rep.* **1**, 287-292.
Sofer, A., Lei, K., Johannessen, C. M. and Ellisen, L. W. (2005). Regulation of mTOR and cell growth in response to energy stress by REDD1. *Mol. Cell. Biol.* **25**, 5834-5845.
Stallaert, W., Dorn, J. F., van der Westhuizen, E., Audet, M. and Bouvier, M. (2012). Impedance responses reveal β_2-adrenergic receptor signaling pluridimensionality and allow classification of ligands with distinct signaling profiles. *PLoS ONE* **7**, e29420.
Teruel, M. N. and Meyer, T. (2000). Translocation and reversible localization of signaling proteins: a dynamic future for signal transduction. *Cell* **103**, 181-184.
Tumaneng, K., Russell, R. C. and Guan, K. L. (2012). Organ size control by Hippo and TOR pathways. *Curr. Biol.* **22**, R368-R379.
Varghese, B. V., Koohestani, F., McWilliams, M., Colvin, A., Gunewardena, S., Kinsey, W. H., Nowak, R. A., Nothnick, W. B. and Chennathukuzhi, V. M. (2013). Loss of the repressor REST in uterine fibroids promotes aberrant G protein-coupled receptor 10 expression and activates mammalian target of rapamycin pathway. *Proc. Natl. Acad. Sci. USA* **110**, 2187-2192.
Vega-Rubin-de-Celis, S., Abdallah, Z., Kinch, L., Grishin, N. V., Brugarolas, J. and Zhang, X. (2010). Structural analysis and functional implications of the negative mTORC1 regulator REDD1. *Biochemistry* **49**, 2491-2501.
Vollmer, J. Y., Alix, P., Chollet, A., Takeda, K. and Galzi, J. L. (1999). Subcellular compartmentalization of activation and desensitization of responses mediated by NK2 neurokinin receptors. *J. Biol. Chem.* **274**, 37915-37922.
Wauson, E. M., Zaganjor, E., Lee, A. Y., Guerra, M. L., Ghosh, A. B., Bookout, A. L., Chambers, C. P., Jivan, A., McGlynn, K., Hutchison, M. R. et al. (2012). The G protein-coupled taste receptor T1R1/T1R3 regulates mTORC1 and autophagy. *Mol. Cell* **47**, 851-862.
Yu, F. X., Zhao, B., Panupinthu, N., Jewell, J. L., Lian, I., Wang, L. H., Zhao, J., Yuan, H., Tumaneng, K., Li, H. et al. (2012). Regulation of the Hippo-YAP pathway by G-protein-coupled receptor signaling. *Cell* **150**, 780-791.
Zacharias, D. A., Violin, J. D., Newton, A. C. and Tsien, R. Y. (2002). Partitioning of lipid-modified monomeric GFPs into membrane microdomains of live cells. *Science* **296**, 913-916.